AD-A139 758 UNDOPED BUFFER LAYER DEVELOPMENT(U) ROCKWELL INTERNATIONAL THOUSAND OAKS CA MICROELECTRONICS RESEARCH AND DEVELOPMENT CENTER D MILLER JAN 84 1/1

UNCLASSIFIED MRDC41086.3FTR AFOSR-TR-84-0231 F/G 20/2 NL

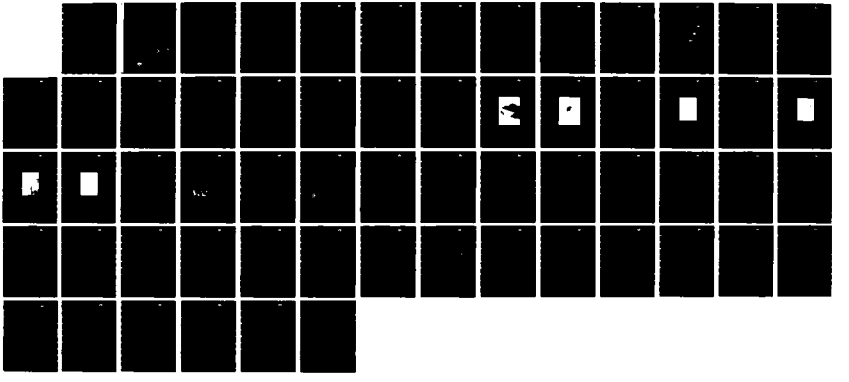

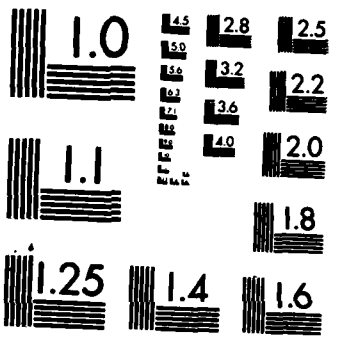

MRDC41086.3FTR
Copy No. 13

UNDOPED BUFFER LAYER DEVELOPMENT

FINAL TECHNICAL REPORT FOR THE PERIOD March 1, 1981 through March 31, 1983

CONTRACT NO. F49620-81-C-0038

Prepared for

Air Force Office of Scientific Research
Building 410
Bolling AFB, DC 20332

D. Miller
Principal Investigator

JANUARY 1984

Rockwell International

Unclassified

SECURITY CLASSIFICATION OF THIS PAGE (When Data Entered)

REPORT DOCUMENTATION PAGE		READ INSTRUCTIONS BEFORE COMPLETING FORM
1. REPORT NUMBER AFOSR-TR- 84-0231	2. GOVT ACCESSION NO. AD-A139758	3. RECIPIENT'S CATALOG NUMBER
4. TITLE (and Subtitle) Undoped Buffer Layer Development		5. TYPE OF REPORT & PERIOD COVERED Final Technical Report 3/1/81 through 3/31/83
		6. PERFORMING ORG. REPORT NUMBER MRDC41086.3FTR
7. AUTHOR(s) D. L. Miller		8. CONTRACT OR GRANT NUMBER(s) F49620-81-C-0038
9. PERFORMING ORGANIZATION NAME AND ADDRESS Rockwell International Microelectronics Research and Development Center, 1049 Camino Dos Rios, Thousand Oaks, CA 91360		10. PROGRAM ELEMENT, PROJECT, TASK AREA & WORK UNIT NUMBERS 61102F, 2306/B1
11. CONTROLLING OFFICE NAME AND ADDRESS Air Force Office of Scientific Research/NE Building 410 Bolling AFB, DC 20332		12. REPORT DATE January 1984 13. NUMBER OF PAGES 59
14. MONITORING AGENCY NAME & ADDRESS(if different from Controlling Office)		15. SECURITY CLASS. (of this report) Unclassified 15a. DECLASSIFICATION/DOWNGRADING SCHEDULE

16. DISTRIBUTION STATEMENT (of this Report)

Approved for public release; distribution unlimited.

17. DISTRIBUTION STATEMENT (of the abstract entered in Block 20, if different from Report)

18. SUPPLEMENTARY NOTES

19. KEY WORDS (Continue on reverse side if necessary and identify by block number)

Epitaxial layer	MBE	Molecular Beam Epitaxy
Undoped buffer layer	MOCVD	Metalorganic chemical vapor deposition
	VPE	Vapor Phase Epitaxy

20. ABSTRACT (Continue on reverse side if necessary and identify by block number)

This program focused on the growth and analysis of epitaxial layers using three different techniques which have been successful in producing high purity, high mobility, epilayer material for device applications. These included molecular beam epitaxy (MBE), metalorganic chemical vapor deposition (MOCVD), and vapor phase epitaxy. Application of characterization techniques such as SIMS (secondary ion mass spectrometry), infrared absorption, photoluminescence, deep level transient spectroscopy, and photoconductivity has allowed (cont.)

DD FORM 1 JAN 73 1473 EDITION OF 1 NOV 65 IS OBSOLETE

Unclassified

SECURITY CLASSIFICATION OF THIS PAGE (When Data Entered)

progress to be made in understanding the major deep impurity centers in semi-insulating epitaxial GaAs.

TABLE OF CONTENTS

Chief, Technical Information Division

LIST OF FIGURES

LIST OF FIGURES

1.0 INTRODUCTION

The importance of material characteristics of semi-insulating GaAs has never been more critical for the fabrication of high performance MESFET devices than it is today. The emergence of a high technology GaAs requirement now reaches to 40 GHz. Direct ion implantation into bulk semi-insulating substrates has shown great promise in the circuit integration area. Many of the highly complex digital logic and memory circuits are now and will be fabricated by direct ion implantation in the future.

It is apparent, however, that other devices, especially in the microwave area, may benefit from high purity epitaxial layers for low noise and/or high power applications. Epitaxial technology has been a mainstay of low noise and high power devices. Future high frequency (> 30 GHz) satellite and secure telecommunications systems may depend upon this well developed technology. However, past progress in epitaxial materials technology has been restricted by a limited understanding and identification of the deep impurity centers present and means for their control.

The purpose of this program has been to produce and analyze epitaxial layers using three different techniques which have been successful in producing high purity, high mobility, epilayer material for device applications. These include molecular beam epitaxy (MBE), metal organic chemical vapor deposition (MOCVD), and vapor phase epitaxy (VPE). Application of characterization techniques such as secondary ion mass spectrometry (SIMS), infrared absorption, photoluminescence, deep level transient spectroscopy and photoconductivity have allowed progress to be made in understanding the major deep impurity centers in semi-insulating epitaxial GaAs.

This report is divided into five main sections. Section 1 is the introduction. Section 2 describes the approach for the growth processes used to produce samples for this program, and contains the discussion of various growth parameters which were investigated. Section 3 presents the results of characterization studies in three parts. The first discusses the differences

in surface morphology. The second part includes the results of SIMS analysis, and the third describes electrical and optical characterization of the epi-layer material. Section 4 describes the results of ion implantation activation studies on the epitaxial layers, and Section 5 presents a summary of the report and contains the concluding remarks.

2.0 EPILAYER GROWTH

2.1 Metallorganic Chemical Vapor Deposition (MOCVD)

2.1.1 Basic MOCVD Techniques

The growth of III-V compounds by MOVCVD was first reported by Manasevit and Simpson in 1969. Since that first report, this technology has been extended to a variety of III-V,II-VI and IV-VI compound semiconductors by a number of researchers. Work at Rockwell by Dupuis and Dapkus has resulted in a wide variety of devices with state of the art performance. Such devices include solar cells, heterojunction lasers, quantum well lasers, heterojunction bipolar transistors, and enhanced electron mobility structures. The material quality has gradualy improved over the years, and these improvements have included the achievement of high purity GaAs with 77K mobility as high as 125,000 $cm^2/V\text{-}s$.

The MOCVD technique as applied to the growth of GaAs employed the metalorganic trimethylgallium and the hydride arsine (AsH_3) as starting materials. The mixture of gases are pyrolyzed in the atmosphere of hydrogen at 600-800°C according to the following reaction:

$$(CH_3)_3Ga + AsH_3 \xrightarrow{H_2} GaAs + 3CH_4 \quad .$$

The growth rate is determined by the mole fraction or partial vapor pressure of the column III metalorganic compounds.

A schematic diagram of the MOCVD reactor typically employed for the growth of GaAs is shown in Fig. 1. Dopant metalorganics TMGa, TMAl, and DEZn are liquids near room temperature with relatively high vapor pressures, and thus H_2 is used as a carrier gas to transport the source vapors into the reaction chamber.

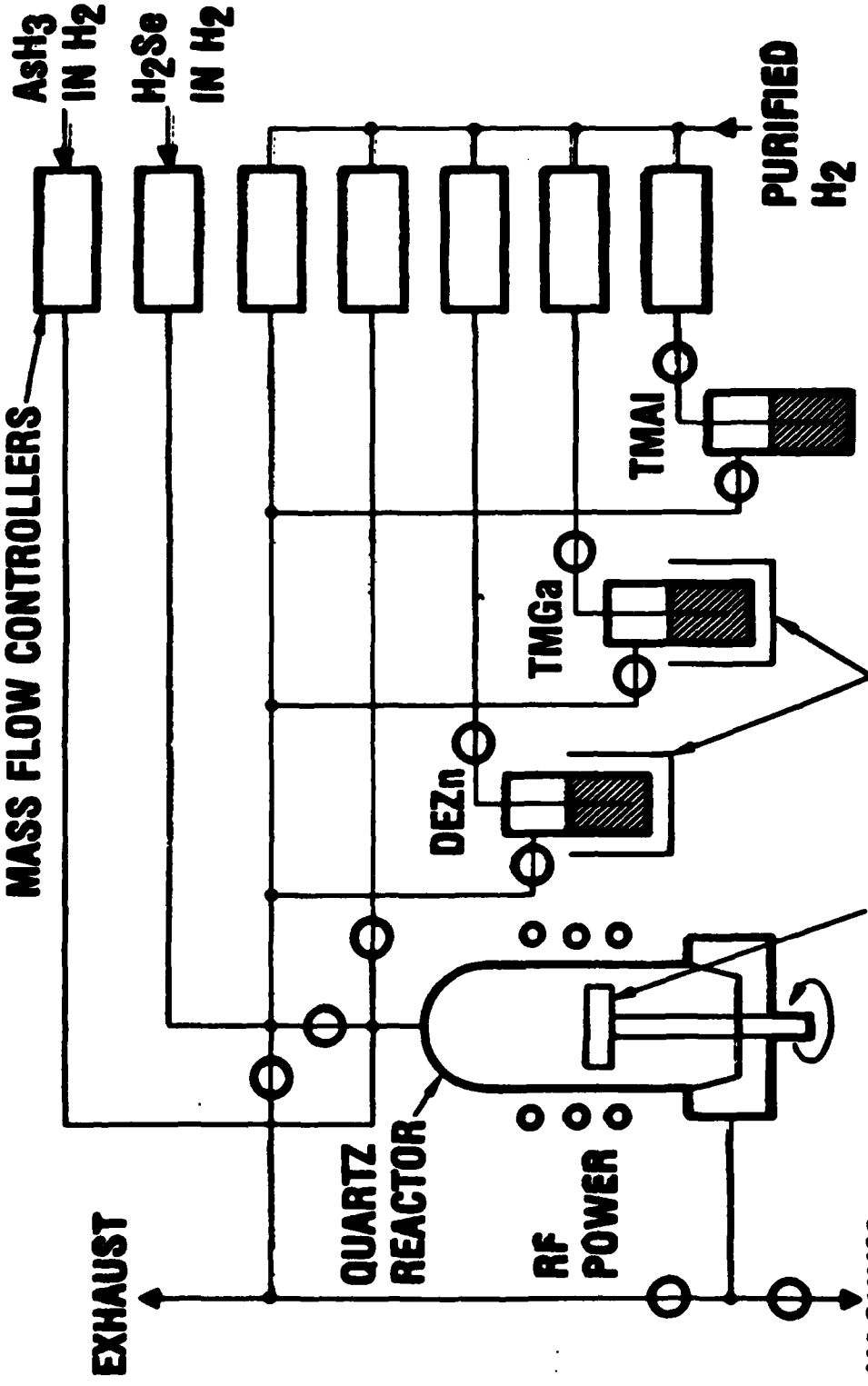

Fig. 1 Schematic diagram of MOCVD reactor.

2.1.2 Crystal Growth Procedure

As described previously, only LEC undoped GaAs substrates were used in these studies. This material has been previously characterized in great detail by a number of techniques including SIMS, photoluminescence, Hall measurement and infrared absorption. MOCVD growth on substrates R38 and R54 (this material was grown and characterized at the Rockwell Thousand Oaks facility) was performed using the following procedure.

First, the substrates were degreased and cleaned following standard procedures. Immediately prior to being introduced into the growth chamber, the substrates were etched to remove surface damage and residual contaminants in either concentrated HCl or in a solution of (5:1:1) H_2SO_4:H_2O:H_2O_2. The substrates weere then rinsed in deionized water, blown dry in dry N_2 gas, and placed on a silicon carbide-coated susceptor in the MOCVD growth reactor. The reactor was then evacuated and backfilled with H_2 purified by diffusion through palladium. The susceptor was next heated by RF induction and temperature monitored with a digital infrared pyrometer. Upon reaching a temperature of 500°C, the arsine flux was started to clean the substrate surface. Growth of GaAs was initiated between temperatures of 600°C and 750°C. Accurate and reproducible gas flows were established with a series of electronic mass flow controllers. Growth rates from 375-1500Å/min were used to grow films 4-5 μm in thickness.

2.1.3 Buffer Layer Growth Parameters

Parameters changed during MOCVD growth included the growth rate, growth temperature and the ratio of arsine to TMGa. As discussed later in this report, the purpose of these changes was to correlate these changes with changes in the electrical and optical properties. Table 1 lists the specific growth parameters used for samples grown during this study.

Table 1

MOCVD Samples
Thickness 4-5 μ for All Samples

Sample #	Growth Rate	Growth Temperature	V/III Ratio
MO-1	0.15 μ/min	625°C	7.5
B21019C	0.15 μ/min	600°C	10.0
B21020C	0.15 μ/min	600°C	12.5
B21206A	375Å/min	625°C	8.0
B30120B	375Å/min	625°C	8.0
B20121A	375Å/min	625°C	10.0
B30228A	375Å/min	620°C	12.0
B30228B	375Å/min	700°C	10.0
B30228C	375Å/min	750°C	10.0

2.2 Molecular Beam Epitaxy (MBE)

2.2.1 MBE Crystal Growth

Nine wafers were grown by MBE for this program. A list of these samples is given in Table 2, together with a summary of growth parameters for each individual sample, and any relevant comments. All samples were grown using a Varian Gen II MBE growth system which was installed in our laboratory in early 1982. The growth process and substrate preparation process were identical to those procedures in use for growing MBE material for several GaAs and AlGaAs device programs with a few exceptions, as noted in this report. Relatively high purity unintentionally doped material could routinely be grown as evidenced by the 77K mobility of modulation-doped material which was routinely above 100,000 cm^2/V-sec. Since this mobility is state-of-the-art for the structures grown, it is believed that these layers are representative of the quality obtainable using commercial MBE machines.

Table 2

Growth Rate 1 μ/h for All Samples
Thickness 3-4 μ for All Samples

Sample #	Substrate	Oval Defect Density (cm^{-2})	Comment
MBV 212	600	2.5×10^3	Foggy
MBV 213	580	2.1×10^3	Foggy
MBV 214	620	1.3×10^3	Foggy
MBV 215	560	4.7×10^3	Foggy
MBV 240	610	1.3×10^3	
MBV 241	600-610	1×10^3	
MBV 242	625	8.4×10^2	
MBV 243	600-605	7.6×10^2	
MBV 244	600-610	8.4×10^2	Bake substrate

To obtain high purity, special care was taken to eliminate initial contamination of the MBE sources. The crucibles used for the Ga and As ovens were pyrolytic boron nitride as supplied by Varian (produced by Union Carbide). These crucibles were boiled for several hours in aqua regia, followed by boiling for several more hours in deionized water before being dried in air and loaded into the system. The crucibles were baked empty in the system for 4 h in the MBE machine under a vacuum of 1×10^{-9} Torr. The ovens were then loaded with 6N Ga (Alusuisse) and 6N As chunks (Cominco), and returned to the MBE chamber. A bakeout of the machine for 48 hours at 170°C was made prior to any growths. Prior to runs #213-#215, 35 μm of material had been grown for other programs. Prior to runs #240-#244, about 70 μm had been grown since bakeout.

The substrates used were from ingots grown in-house at Rockwell from two semi-insulating boules of LEC GaAs, R38 and R54. Initial resistivity measurements on test wafers from these boules indicated resistivities of 2×10^8 ohm-cm and 9×10^7 ohm-cm, respectively. Etch pit densities were about 1.5×10^5 cm^{-2} and 5×10^4 cm^{-2}, respectively. Wafers from these ingots were polished using a chemical-mechanical polishing procedure which leaves a flat, specular, nearly damage free surface. The backside of the wafers were coated with silicon nitride to protect them from attack by In used to fasten the substrates to the mounting block in the MBE machine. The front surfaces were etched for 15 sec in agitated hot H_2SO_4:H_2O:H_2O_2(7:1:1) to remove residual damage, rinsed with H_2O, and blown dry with dry N_2 gas. These substrates were mounted with In on Mo substrate holders supplied by Varian. Just prior to insertion into the MBE system, the substrate were etched on a low speed spinner with flowing NH_4OH:H_2O:H_2O_2 (10:1:1) for 15 sec, rinsed with H_2O, and spun-dry in air to complete the preparation procedure.

Substrates and holders were degassed in the preparation chamber of the MBE machine prior to insertion in the growth chamber. The remaining oxide was thermally desorbed in an As_4 flux prior to growth. All ion guages and electron beams in the growth chamber were off during growth of the layers for this program.

The growth parameters varied were the substrate temperature and surface pretreatment. The substrate temperature was varied from run to run to investigate the effect of this parameter on buffer layer properties. Substrate temperature was measured with an optical pyrometer (IRCON model 2000), calibrated by observing the formation of the Si-Al eutectic at 577°C on Si test wafers mounted on the substrate holder during a separate calibration procedure.

One substrate (for run #244) recieved a special prebake treatment for 7.5 hours at 750°C in UHP H_2. This process has been reported to result in reduced impurity diffusion into MBE epilayers grown on Cr-doped substrate material. Following this treatment, the wafer had partially decomposed. The

wafer was repolished and etched to remove several microns near the surface. The rest of the substrate preparation was identical to that described above.

Typical growth rates were 1 μm.h with an As/Ga beam equivalent ratio (as measured by the beam flux monitor of the GEN II machine) of about 35. This resulted in As-stabilized growth ,although for the higher substrate temperatures the growth was very close to being Ga-stabilized. This resulted in a slight haziness on several wafers, as noted in Table 2.

2.3 Vapor Phase Epitaxy

2.3.1 VPE Crystal Growth

The epitaxial process proposed for this program was selected on the basis of:

1. Highest known purity.
2. Demonstrated most useful in present buffer layer and multilayer growth.
3. Basic process with fewest variables for research study.

The $AsCl_3GaH_2$ process was selected because of its inherent simplicity in performing high purity epitaxy with the fewest chemical variables. The key features of the process are:

1. High Purity Aspects

   a. Performs a direct synthesis of GaAs and epitaxial growth by vapor transport.
   b. All chemical agents and elements are of the best available purity (7-9s) with excellent availability.

1) Segregation of n- and p-type impurities in Ga/GaAs source. GaAs crust forms by a solution growth method producing a very pure GaAs source for transport.

Hydrogen used for transport is purified by diffusion through a Pd-Ag membrane to reduce O_2 and H_2O to concentrations below 0.1 ppm. Mass flow controllers are used to regulate all hydrogen and dopant flow in the reactor for accurate and reproducible control of epitaxial growth rate. The $AsCl_3$ buffers are constructed from pyrex and utilize a reflux design, which allows accurate and reproducible control of the $AsCl_3$ partial pressure necessary for both GaAs transport and Si suppression during buffer layer growth.

2.3.2 $AsCl_3$ VPE Technology

Since the initial work with $AsCl_3$ VPE by Mehal, many improvements and modifications have been made to the original VPE process. The growth apparatus shown in Fig. 2 has been developed to produce multilayers of high purity and controlled doping for MESFET applications. The properties of the reactor are detailed below.

Growth Mode:	Kinetically controlled growth regime.
Thermal Profile:	Flat profile type, uniform source and substrate zone (< 0.2°C/cm).
$AsCl_3$ Control:	Reflux type source for precise control of $AsCl_3$ mole fraction.
Growth/Source Temperatures:	Growth Zone: 760°C, Ga source zone: 820°C.
Epitaxial Growth Rate:	0.1-0.1 μm/min.

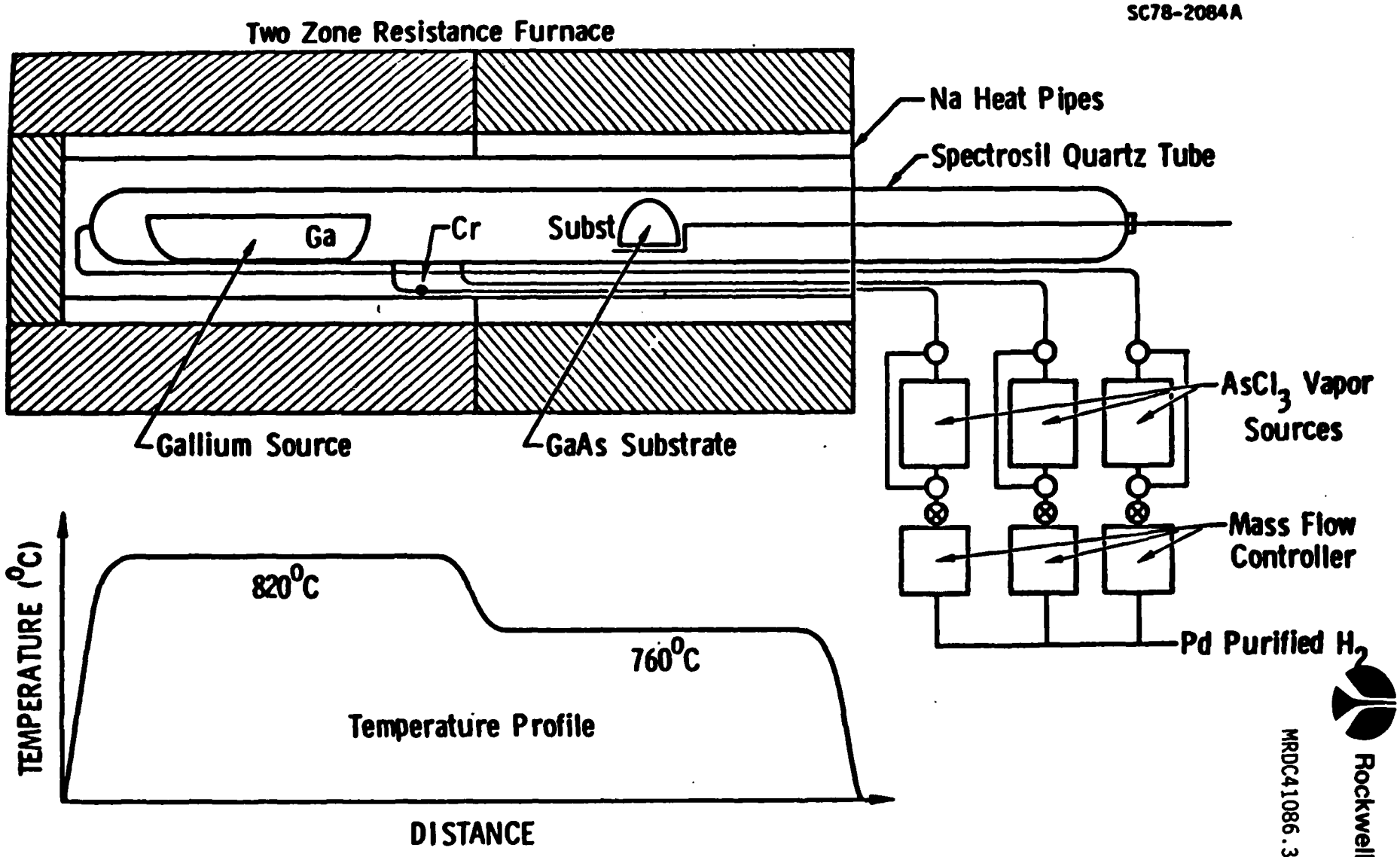

Fig. 2 $AsCl_3$ VPE growth apparatus.

The reactor can be brought to rapid thermal equilibrium with the rolling, preheated furnace equipped with Na filled heat pipes to provide an extremely uniform thermal geometry for vapor transport and epitaxial growth. The reactor tube is constructed from Spectrosil fused silica to reduce exposure to the metallic impurity oxides of Fe, Mg, Ca and Ti found in laboratory grade silica. All aspects of the reactor have been studied carefully over the past ten years to provide extremely laminar gas flow for a uniform deposition regime. A careful compromise between the Ga source and substrate deposition temperature were determined to both limit the activity of Si in the Ga source due to solubility, and reduce the net deposition rate to that useful in producing submicron thick layers. Extensive studies of auto doping have been conducted in the past to allow growth to clean well-ordered substrate/epitaxial layer interfaces with minimum contributions from substrate dopants.

2.3.3 Epitaxial Growth Procedure

The epitaxial reactor is prepared by first determining the leak integrity with a vacuum-helium leak detector to $< 10^{-9}$ cc/sec. High temperature baking in H_2 (850°C) is performed to remove absorbed moisture.

The Ga (7-9s) is also baked out, but at a lower temperature (820°C) for 12 hours prior to saturation with As. Removal of residual moisture is important in assuring high carrier mobilities, free of compensating effects.

Following As saturation by transport of $AsCl_3$:H_2 mixtures, the reactor is ready for use in epitaxial growth. The operation sequence for epitaxial growth is outlined below:

1. Sample loading and purging.
2. Thermal equilibrium to operating temperature.
3. GaAs source saturation, vapor etching of sample.
4. Initiation of epitaxial growth/termination of growth.
5. Removal of furnace/cool to room temperature/unload.

Modifications to the above procedure are made to incorporate dopants via gas phase by use of solid sources (Cr, Fe) or gas mixtures (H_2S, SiH_4). Table 3 lists the samples and growth parameters of VPE layers grown for this contract.

Table 3

Sample	Type	Approximate Net Doping	Layer Thickness	Substrate	$\chi AsCl_3 \times 10^3$
1352	p-	$< 10^{13}$ cm^{-3}	21 μm	R7/C(1)	11.8
1361	p-	$< 10^{13}$ cm^{-3}	35 μm	χS-254(2)	11.8
1361	p-	$<< 10^{13}$ cm^{-3}	40 μm	C3-28(1)	10.1
1381	n	$\sim 10^{14}$ cm^{-3}	24 μm	C3-28	9.0
1362	p-	$<< 10^{13}$ cm^{-3}	5 μm	G-22-14H(2)	10.6

(1) Undoped LEC substrates
(2) Cr doped horizontal Bridgman substrates.

3.0 CHARACTERIZATION

A number of measurements were made to characterize the samples grown in this study. These included investigations of the surface morphology, chemical analysis, electrical measurements and various optical measurements. Selected samples were ion implanted to test their suitability for such processing. The following sections detail the results of these measurements. The goal was to identify defect states and impurities which affected sheet resistance and the electrical properties of the material, and to identify those properties of the material such as implant activation which would play a role in determining device characteristics.

3.1 Morphology

3.1.1 MBE Material

The majority of the are of these runs was (as-grown) smooth, flat and featureless. However, all wafers contained the oval-shaped blemishes common to MBE growth, usually referred to as "oval defects" or "coffee bean" defects. Examples of these are shown in Figs. 3 and 4. The density of these defects ranged from 760 cm^{-2} to 470 cm^{-2}. The origin of these features is not understood and they have not yet been eliminated. Their effect on electrostatic or transport properties of the epitaxial material is also not known.

On several of the wafers, a slight haziness was observed. Under high magnification, this haziness can be resolved as a rippled surface morphology. These ripples are characteristic of a low As/Ga flux ratio for the substrate temperature used, which results in nearly Ga-rich growth. This morphology seems to have little effect on the properties of GaAs.

3.1.2 MOCVD Material

All films grown in this study show reflection morphology typical of GaAs grown on GaAs. In general, the morphology improves with the increase in

MRDC84-25400

Fig. 3 SEM photograph of oval defects.

MRDC84-25401

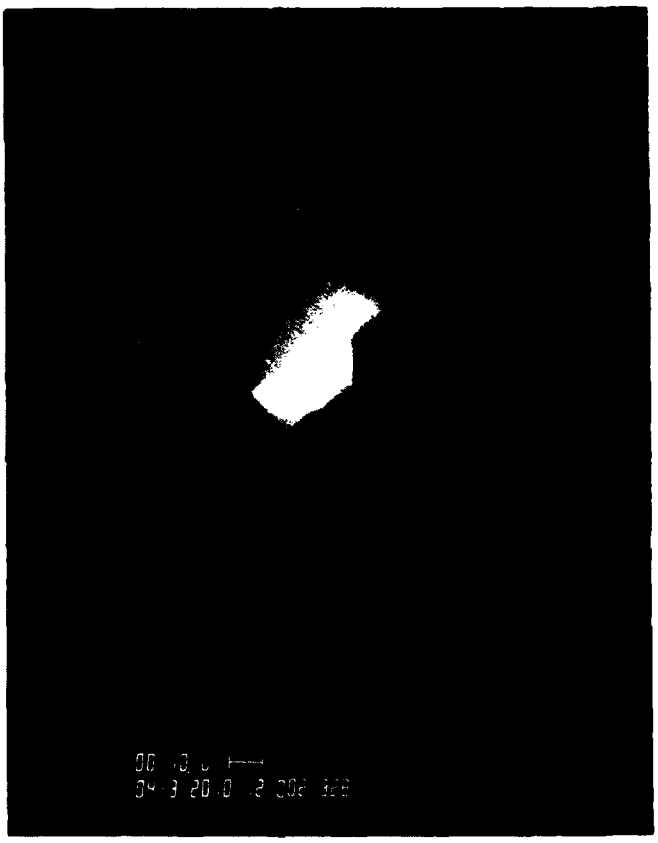

Fig. 4 SEM photograph of oval defects.

growth temperature from 620°C to 750°C, as shown in Figs. 5 - 7, and the number of defects are substantially reduced.

Another strong factor affecting the morphology is the rate of growth. The lower growth rate, the smoother the morphology, as illustrated in Figs. 8 and 9.

In terms of defects, it should be noted that the shape and density of the defects are strongly dependent on the growth parameters, but no strong correlation between the type of defects observed and the growth parameters can be drawn with the limited available data.

3.2 Chemical Analysis

Chemical analysis was made on a number of selected samples using secondary ion mass spectroscopy (SIMS). The SIMS analyses were performed by Charles Evans and Associates. The SIMS measurements were concentrated on the elements Fe, Cu, Mn, B, Ni, Cr and Mg which are common residual impurities found in GaAs. Of these, Fe, Cu, Mn, Ni and Cr are known to be fast diffusers in GaAs under some circumstances, and can thus easily be incorporated into the epilayer from the substrate or from absorbed species on the semiconductor surface. Boron (B) diffuses slowly in GaAs and is used as a marker between the substrate and epilayer. Table 4 lists the samples on which SIMS measurements were made. The table includes four samples grown by MBE, four grown by MOCVD, and four which were implanted, capped with sputtered silicon nitride and annealed. Of these four, two were grown by MOCVD and two were grown by MBE.

Figs. 10 - 17 show the SIMS profiles obtained on the as-grown layers. Figure 18 shows results for a reference sample. The results on the reference sample may be taken as representative of the background sensitivity of the SIMS measurement. There is typically an uncertainty of a factor of two on the concentration scale and 7% on the depth scale. Each of the samples is between 4 and 5 μm thick which agrees with the estimated growth rates. Most of the samples show some contamination at the initial growth interface. MBE samples show small amounts of Fe and Ni. MOCVD samples are frequently contaminated by

MRDC84-25397

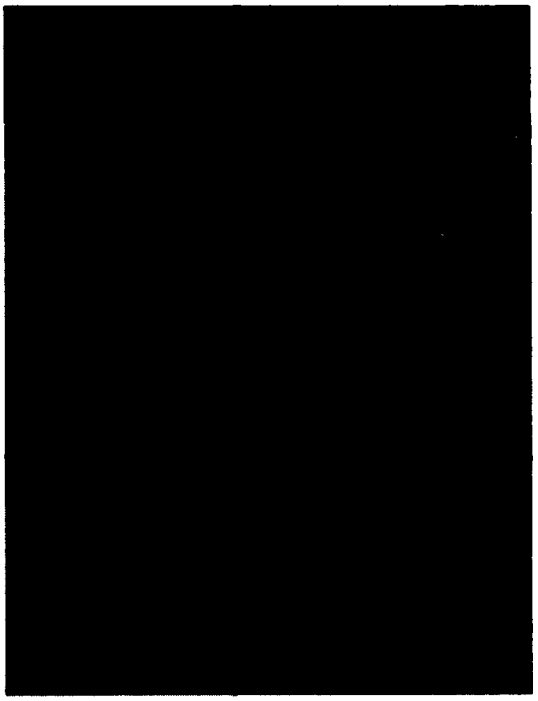

Fig. 5 Surface morphology of MOCVD sample, growth temperature = 620°C.

MRDC84-25395

Fig. 6 Surface morphology of MOCVD sample, growth temperature = 700°C.

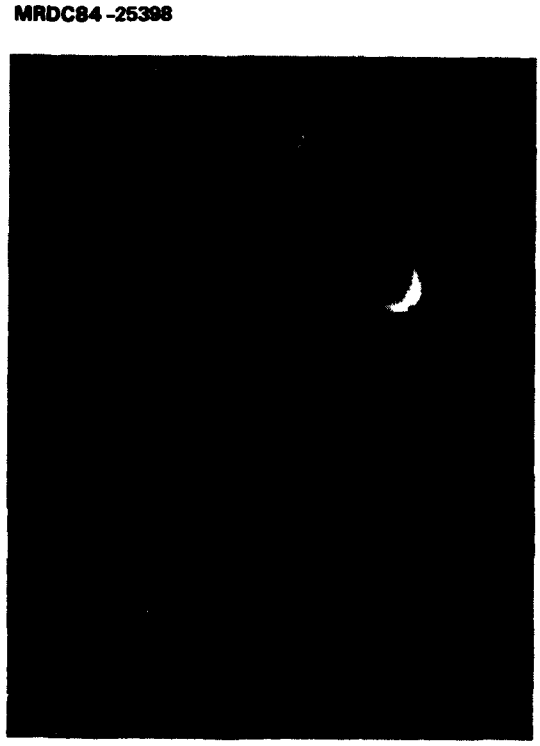

Fig. 7 Surface morphology of MOCVD sample, growth temperature = 750°C.

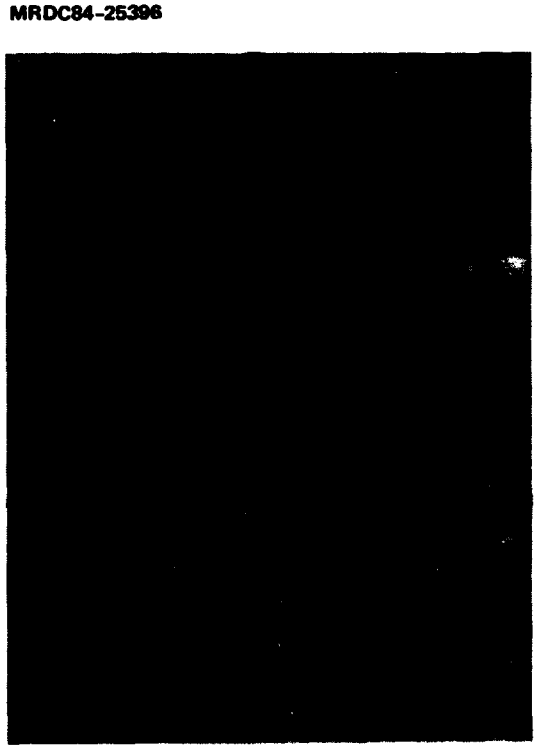

Fig. 8 Surface morphology of MOCVD sample, growth temperature = 375 Å/min.

MRDC84-25399

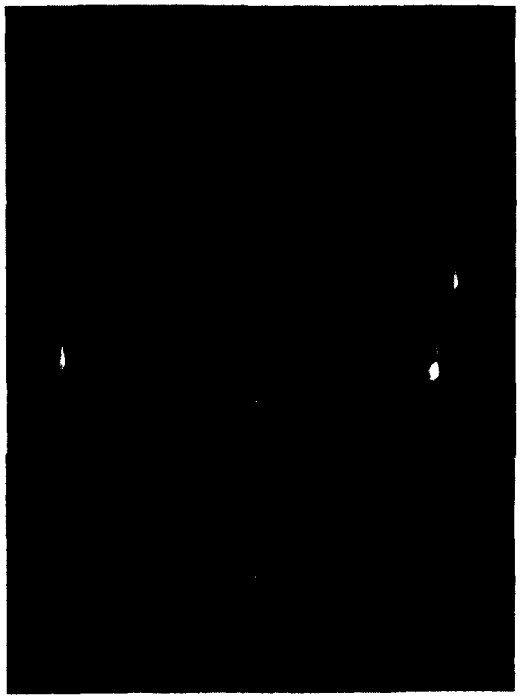

Fig. 9 Surface morphology of MOCVD sample, growth temperature = 1500 Å/min.

Table 4

Samples for SIMS Measurements

Sample	Growth Method	Growth Temperature	Comments
MBV215	MBE	600°C	Foggy
MBV214	MBE	620°C	Foggy
MBV243	MBE	600-605°C	
MBV244	MBE	600-610°C	Baked substrate
B30120B	MOCVD	625°C	
B21010C	MOCVD	600°C	
B30228B	MOCVD	700°C	
B30228C	MOCVD	750°C	
MBV215-Se	MBE	600°C	Se^+ implant 850°C 30 min anneal
MBV243-Se	MBE	600-605°C	Se^+ implant 850°C 30 min anneal
B30120B-Se	MOCVD	625°C	Se^+ implant 850°C 30 min anneal
B30228B-Se	MOCVD	700°C	Se^+ implant 850°C 30 min anneal
C_I'			implant control

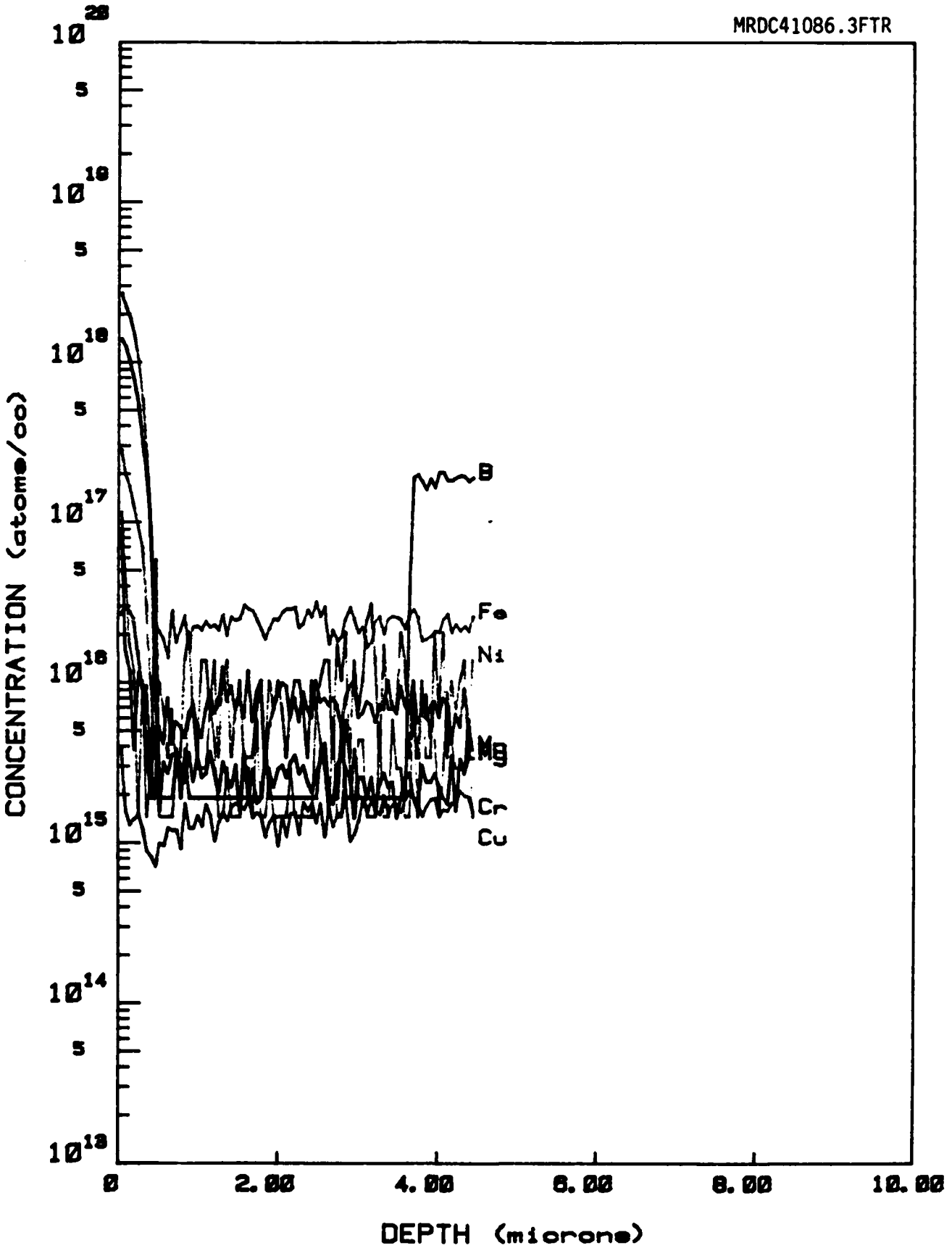

Fig. 10 SIMS profile, sample MBV 215.

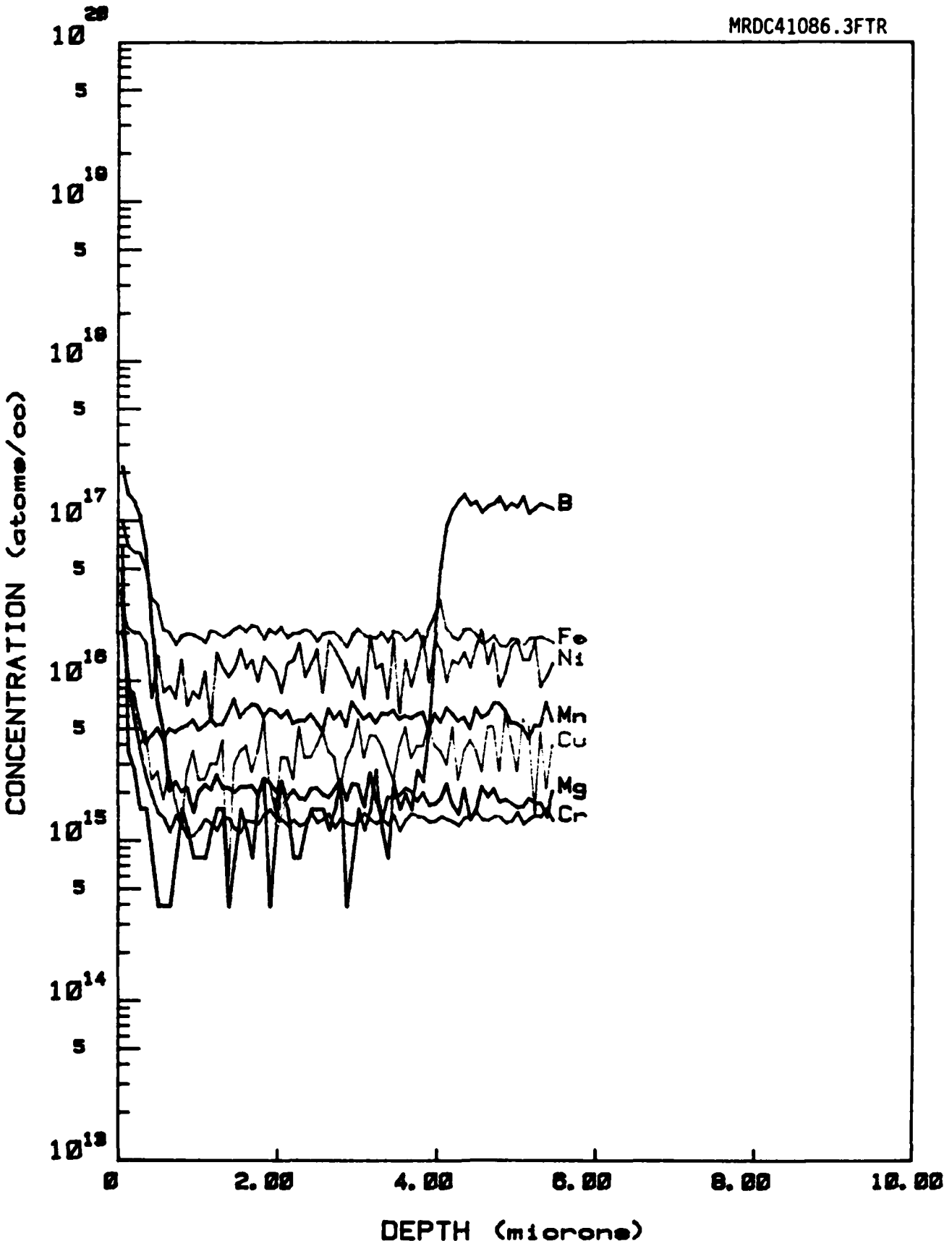

Fig. 11 SIMS profile, sample MBV 214.

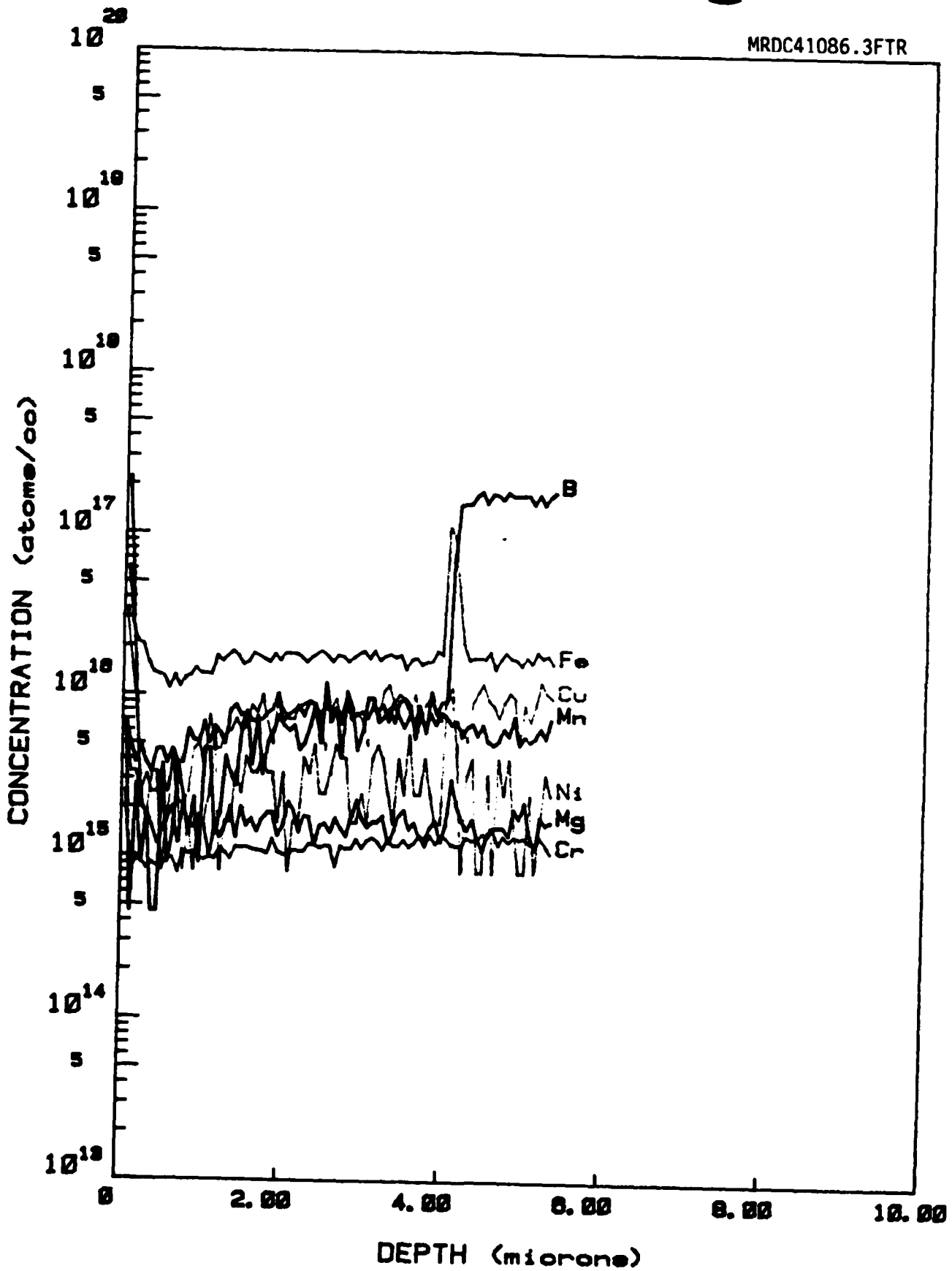

Fig. 12 SIMS profile, sample MBV 243.

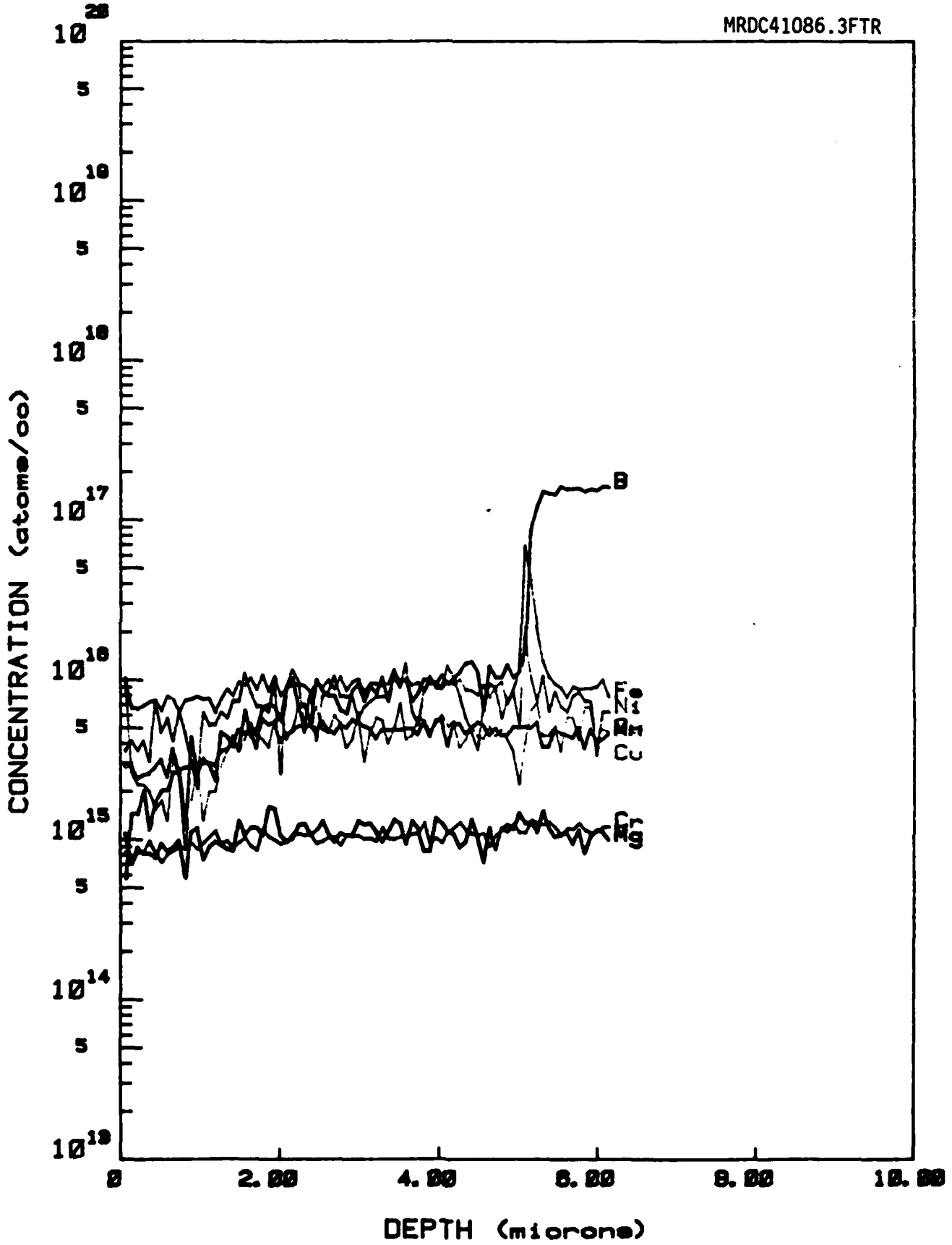

Fig. 13 SIMS profile, sample MBV 244.

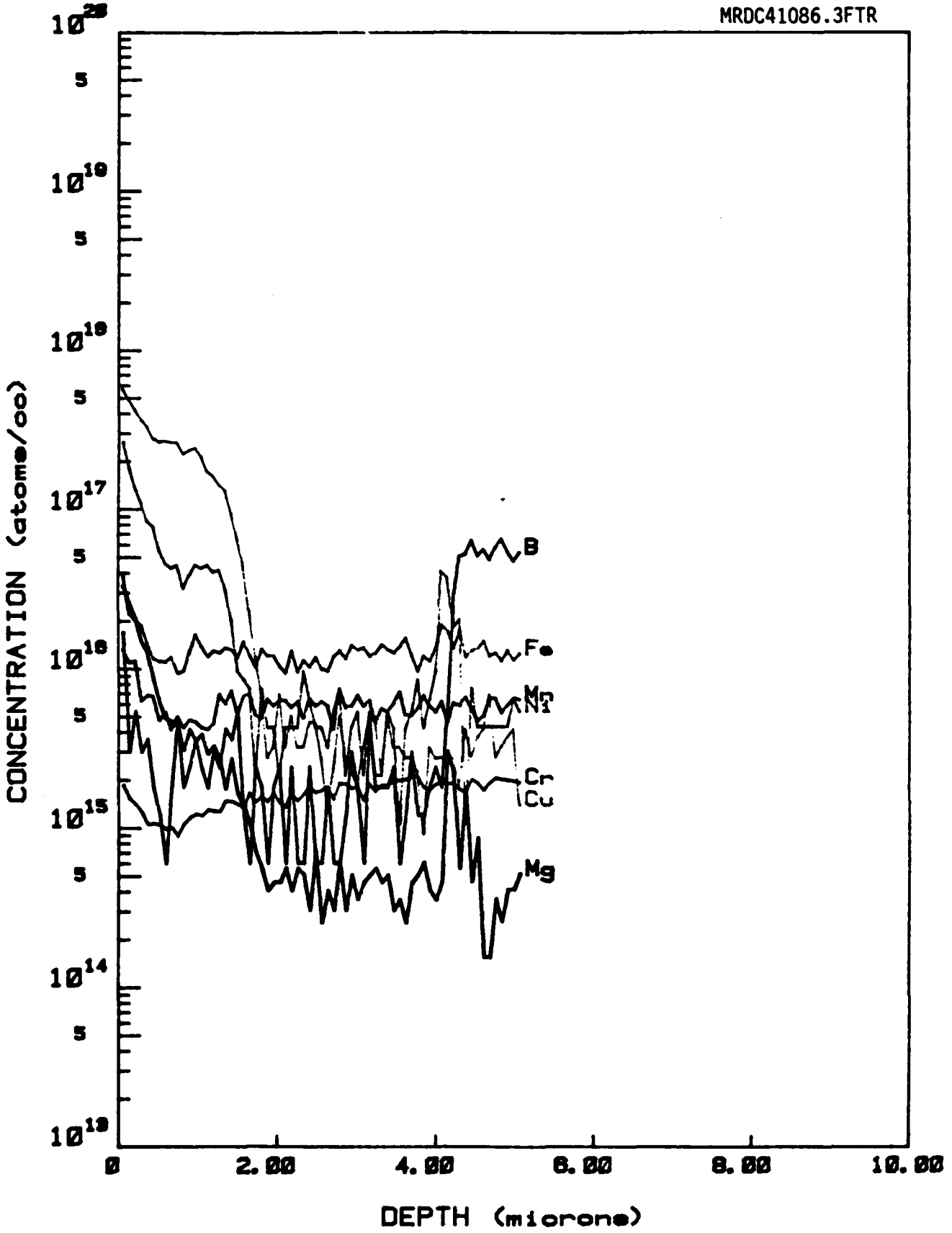

Fig. 14 SIMS profile, sample B30120B.

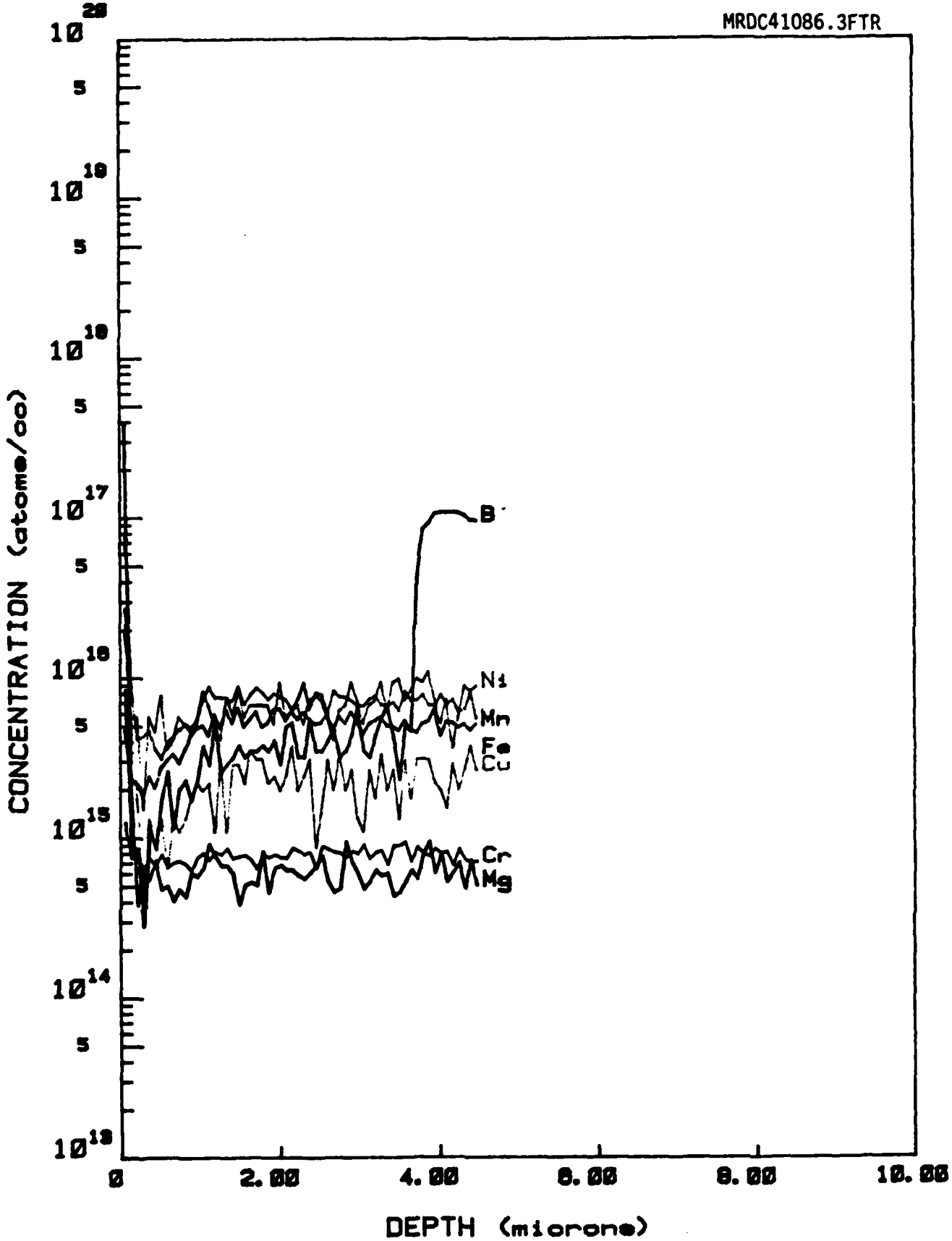

Fig. 15 SIMS profile, sample B21010C.

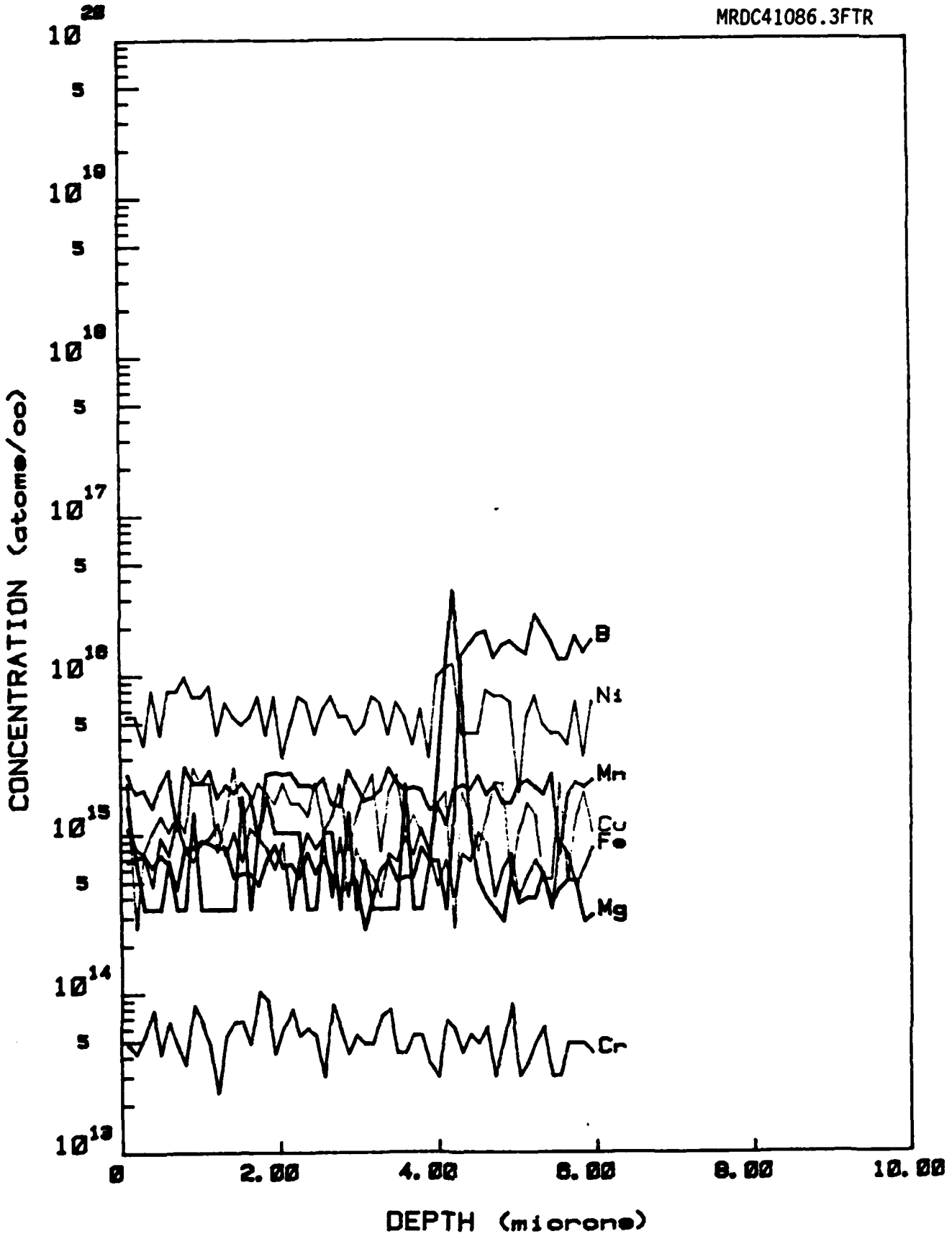

Fig. 16 SIMS profile, sample B30228B.

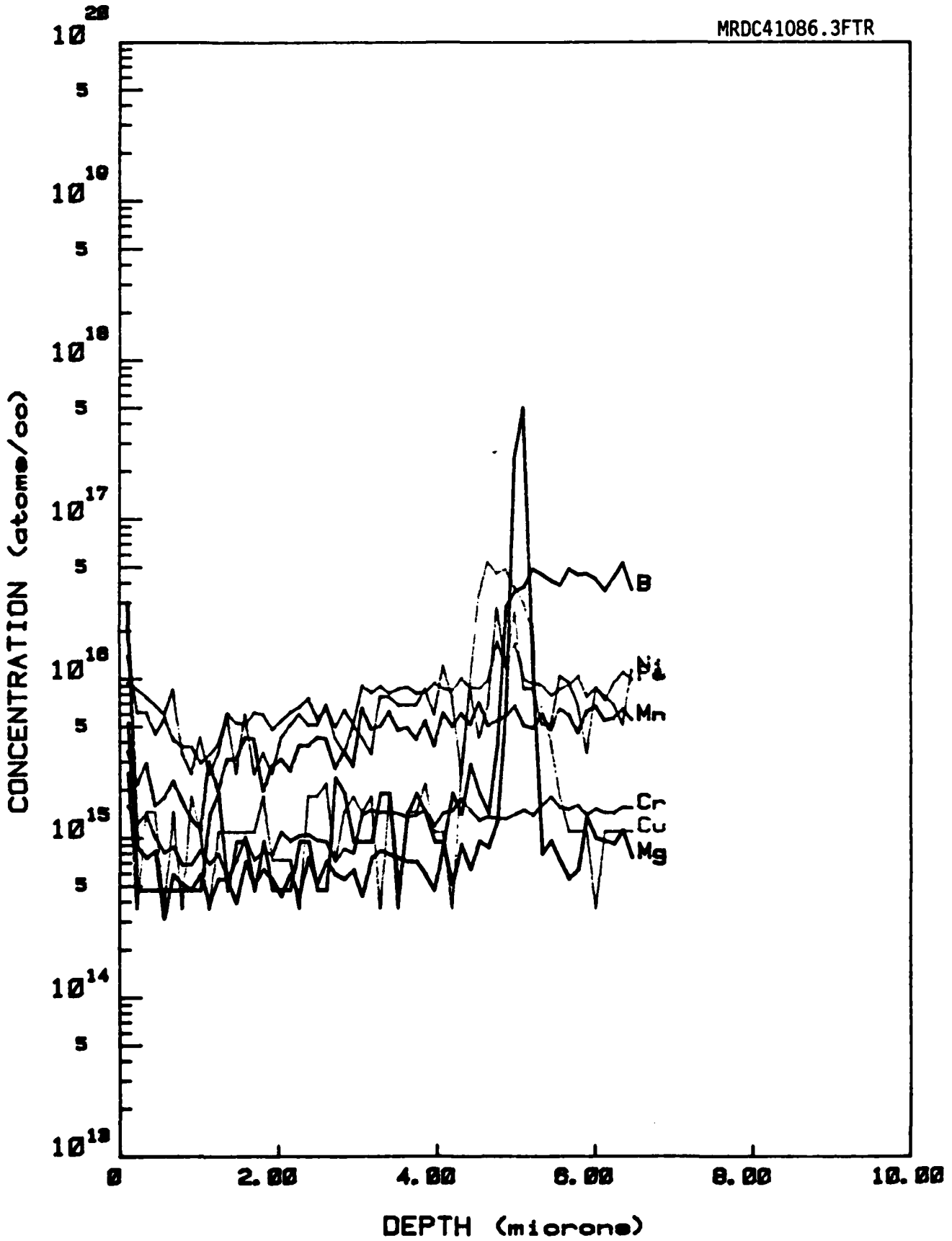

Fig. 17 SIMS profile, sample B30228C.

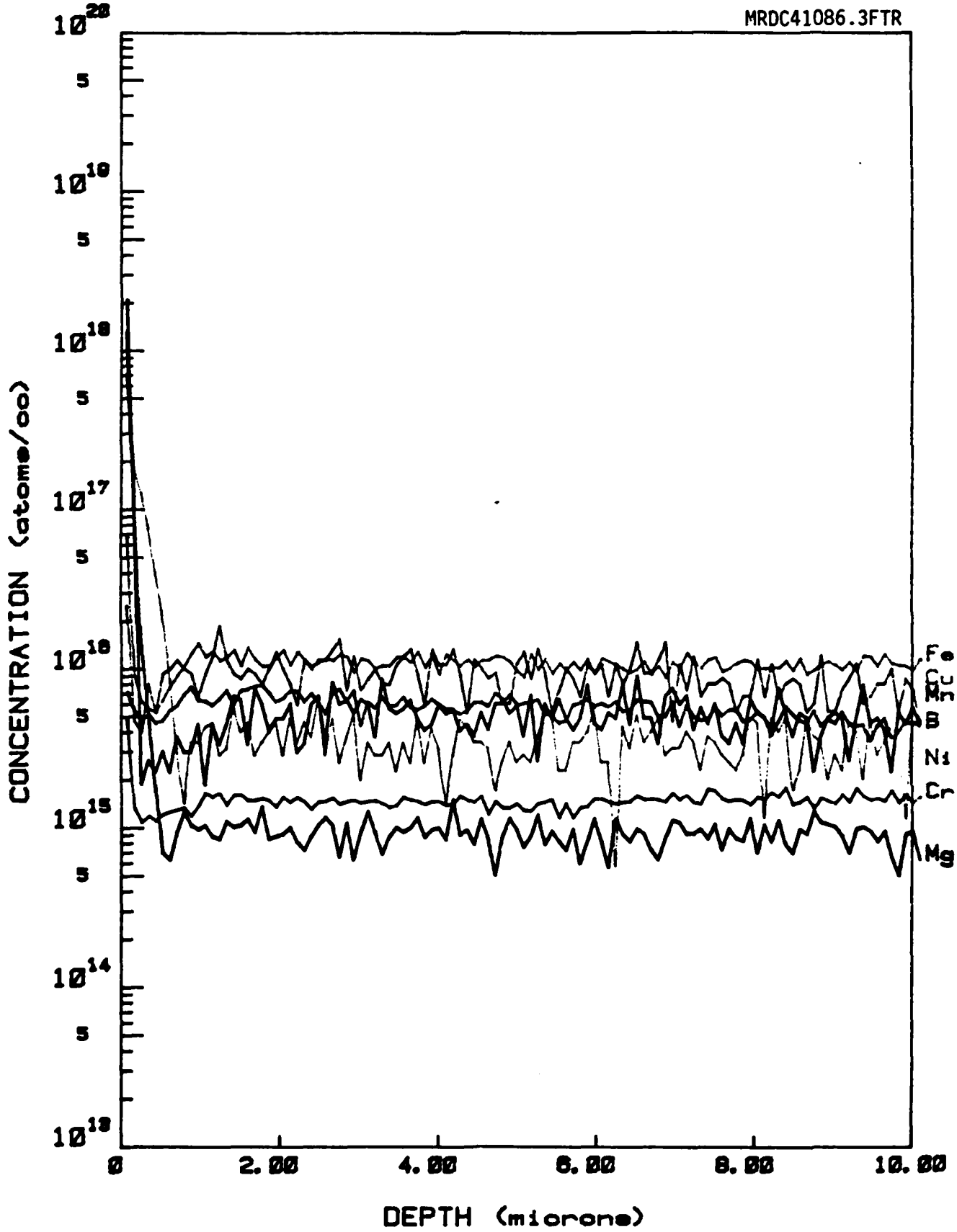

Fig. 18 SIMS profile - background reference.

Cu, Ni, and large amounts of Mg or C_2(molecular carbon). The contamination is typically less for the MBE samples than for the MOCVD samples.

Since the contamination differs between MBE and MOCVD samples, we can eliminate the substrate as the source of the contamination. Some samples such as MBV215 grown by MBE and B21020C grown by MOCVD show no evidence of contamination at the interface. This conclusion is substantiated by the fact that the substrate material was from the same ingot for these runs as for other runs which did show contamination.

A more likely explanation is that this contamination is introduced during the initial surface preparation procedure. The source of such contamination can only be speculated on at this point. Although a substantial amount of contamination occurs at the interface, we do not observe a large amount of contamination throughout the epilayer itself. However, the presence of such contamination raises some questions regarding the ultimate purity obtained in the epilayer material.

The results of the SIMS measurements on the implanted and annealed samples are discussed in the section dealing with ion implantation studies. In short, these studies indicate the presence of a higher degree of contamination in the implanted layers.

3.3 Electrical and Optical Measurements

3.3.1 Hall Measurements

Room temperature Hall measurements were made on each sample grown for this study to determine the carrier concentration, conductivity type, and effective mobility in the undoped layers. The results of these measurements are shown in Table 5. Also listed in Table 5 are the growth temperature and, when applicable, the III/V incident flux ratio. A number of points should be made concerning the Hall measurements. The measured values shown in Table 5 have been calculated using the actual thickness of the epilayer. It has been assumed that the conductivity of the substrate is negligible. These assumptions are

Table 5

Sample No.	Type	Density (cm^{-3})	Mobility	Growth Temperature	III-V Ratio
MBV212	p	1E13	350	600	-
MBV213	p?	< 5E13	< 300	580	-
MBV214	p	5E13	< 300	620	-
MBV215	p	2.7E14	436	560	-
MBV240	p	1E14	55	610	-
MBV241	p	5E14	320	600-610	-
MBV242	p	5E14	300	625	-
MBV243	n	3E15	2250	600-605	-
MBV244	p	5E14	380	600-610	-
M01	p	1.4E15	330	625	7.5
B21019C	p?	5E14	361	600	10.0
B21020C	p	1E15	333	600	12.5
B21206A	p	1E15	423	625	8.0
B30120B	p	< 1E13	< 200?	625	8.0
B20121A	p?	< 1E13	< 100?	625	10.0
B30228A	n?	< 1E14	~ 1000	620°C	12.0
B30228B	n	< 1E12	~ 3600	700°C	10.0
B30228C	n	1.2E15	5000	750°C	10.0

only valid for carrier concentrations in excess of 1×10^{14} cm^{-3}. At lower carrier concentrations, surface depletion becomes important and the epilayer becomes depleted. Therefore, the only information which can be obtained from the Hall measurements is a rough measure of the carrier concentration. In most of the MBE grown samples and in some of the MOCVD samples, the conductivity is p-type and the carrier concentration is in the range of 1×10^{14}. In many of the remaining samples, the conductivity was indeterminate due to the low conductivity. The low conductivity, as stated above, indicates that the carrier concentration is less than 1×10^{14}. In virtually all cases, the residual conductivity was nonuniform across a sample and extremely light sensitive. Such behavior is to be expected when the epitaxial layer is almost pinched off. Two buffer layers, B30228B and B30228C, grown at higher temperature were n-type. This may have been a result of outgassing of residual dopants at the higher temperature or simply a memory effect in the system from previous doped runs. Further characterization studies did not reveal the dopant.

Undoped buffer layers grown by VPE are listed in Table 3. Since these layers were somewhat thicker than the layers grown by MBE and MOCVD carrier concentrations as low as 10^{13} could be measured. As in the case of material grown by MBE or MOCVD, most of the layers were lightly p-type although at least one layer was n-type.

3.3.2 Trapping Measurements

On selected samples, a number of measurements were performed in an effort to determine the presence of residual trapping centers in the epilayers which were grown under this program. These measurements included photo-induced transient spectroscopy (PITS), deep level transient spectroscopy (DLTS) and infrared photoconductivity. For the most part, these studies were unsucessful in detecting residual traps in the epilayers.

PITS measurements were made on a number of samples, and a number of transient photoconductive effects were observed. However, these effects could be associated with photoconductive processes in the substrate material involving the deep trap EL2. EL2 is the principal defect occuring in the substrate mate-

rial and is responsible for the semi-insulating behavior of undoped LEC GaAs. Although additional structure was observed in the PITS spectra, additional structure was not sufficiently regular for reliable interpretation.

AC admittance measurements were attempted on some of the more conducting undoped samples. Series resistance dominated the electrical properties of devices fabricated for these measurements and no indications of trapping levels were observed. Normal pulsed capacitance DLTS measurements were not possible because of similar problems with series resistance in the devices.

Infrared photoconductivity measurements were made on selected samples in the mid-infrared (3-20 um) with a Nicolet MX-1 Fourier Transform Spectrometer. Near-infrared photoconductivity measurements (1-3 μm) were made using a conventional spectrometer. No photoconductivity was observed for wavelengths longer than 1.6 μm. At shorter wavelengths, photoconductivity characteristic of EL2 was observed. This photoconductivity is most likely related to the underlying substrate material. As stated previously, EL2 is the dominant defect species in the substrate.

3.3.3 Photoluminescence Measurements

Photoluminescence measurements at 77K were performed on selected samples to determine the presence of residual impurity levels and contaminants. These samples included MBE material, MOCVD material and samples which had been ion implanted and annealed. Figs. 19 - 24 show representative spectra obtained in MBE and MOCVD material, respectively. The data on ion implanted material is discussed in Section 4. Each of the spectra shows bandedge luminescence near 8200A. At lower energies we observe luminescence from residual impurities and traps. We should note that this luminescence is characteristically different in the MBE and MOCVD material. In the MBE material we observe two additional bands. One of these peaks at 9100A and is not observed in the MOCVD material. It is believed that this band is associated with a Cu-containing complex. The second band occurs at 1.5 μm and its origin is unknown. The deep donor EL2 gives rise to luminescence which typically peaks at longer wavelengths. The The following figures will each have a separate page at final printout.

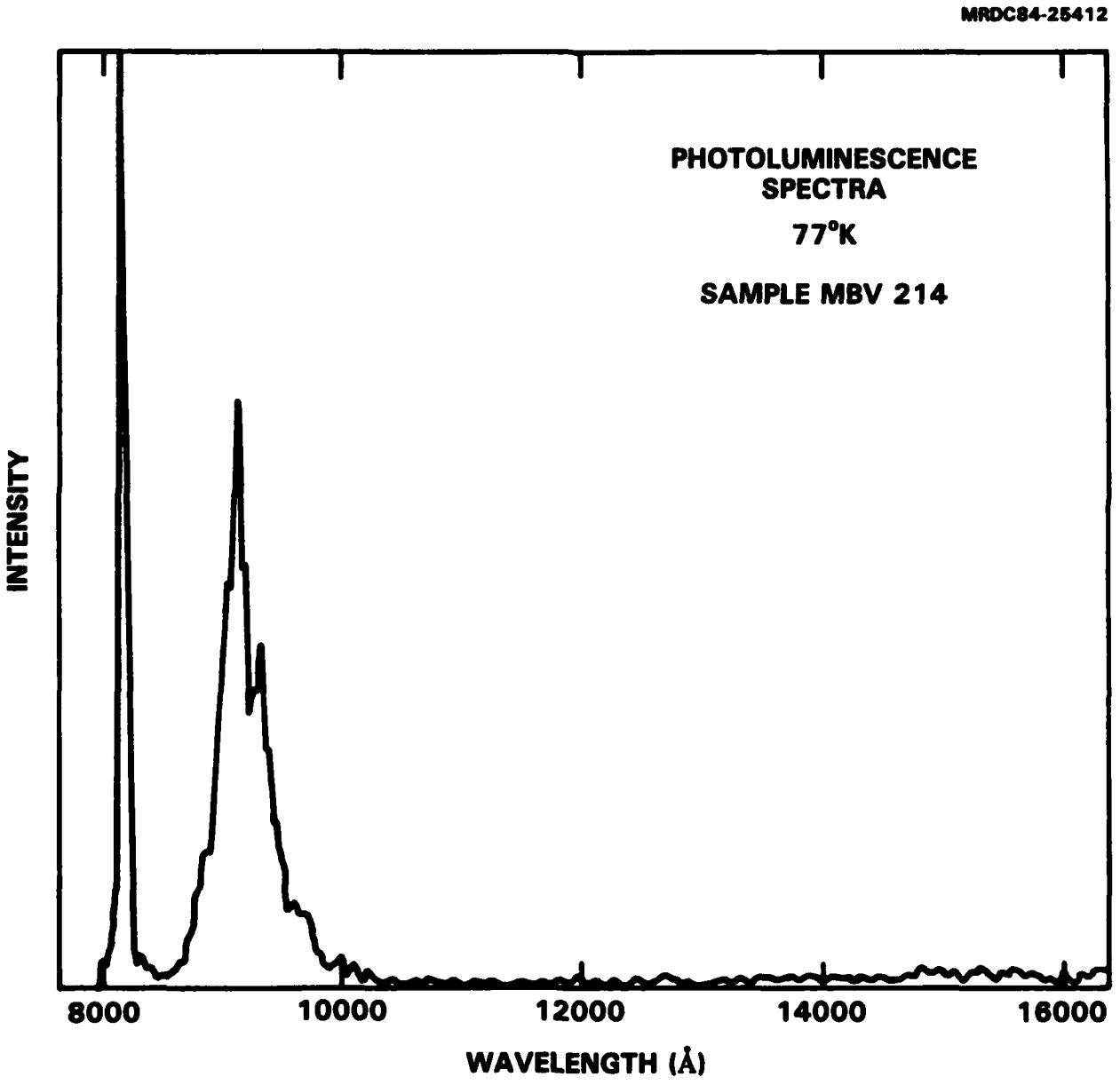

Fig. 19 Photoluminescence spectra, sample MBV 214.

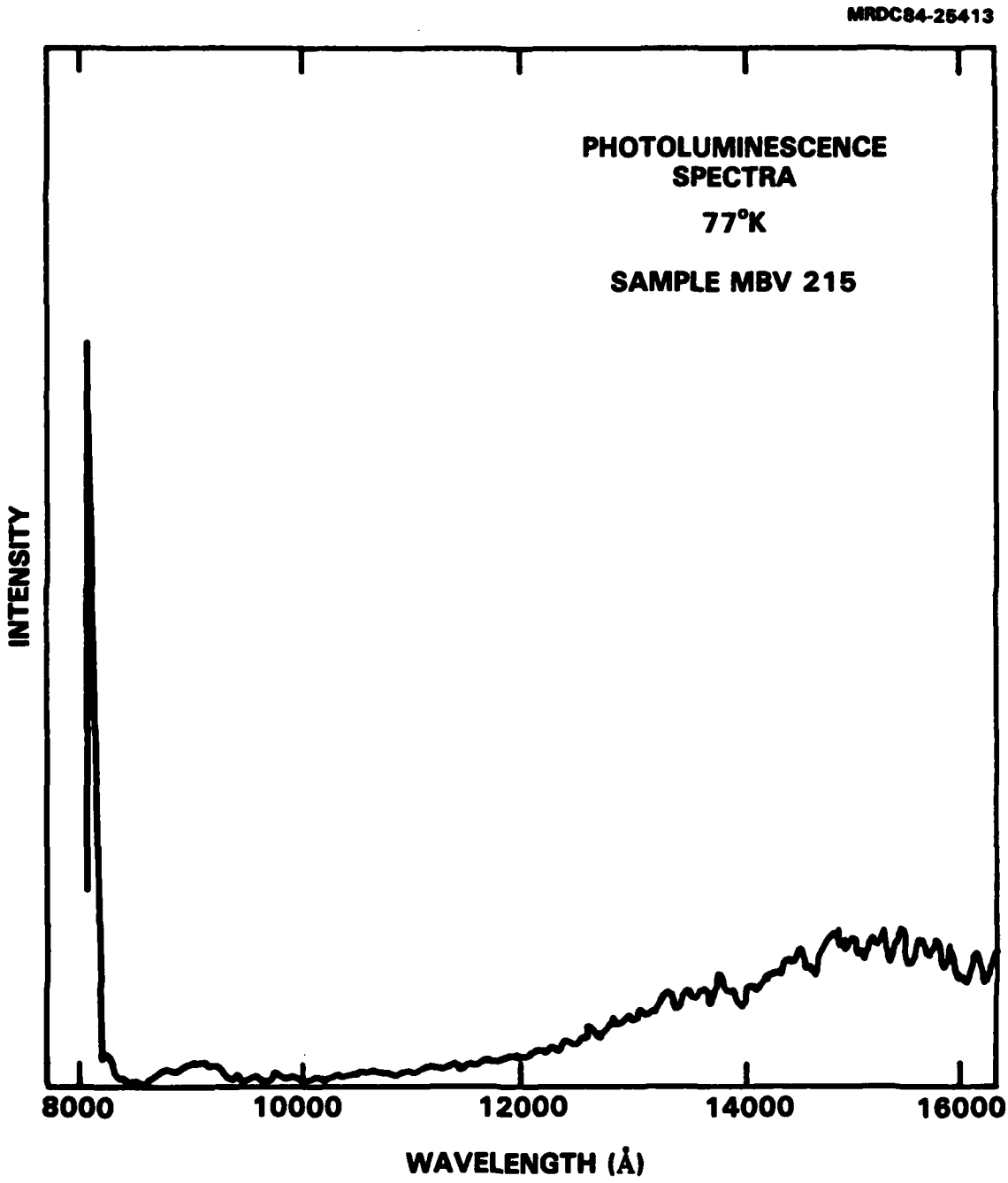

Fig. 20 Photoluminescence spectra, sample MBV 215.

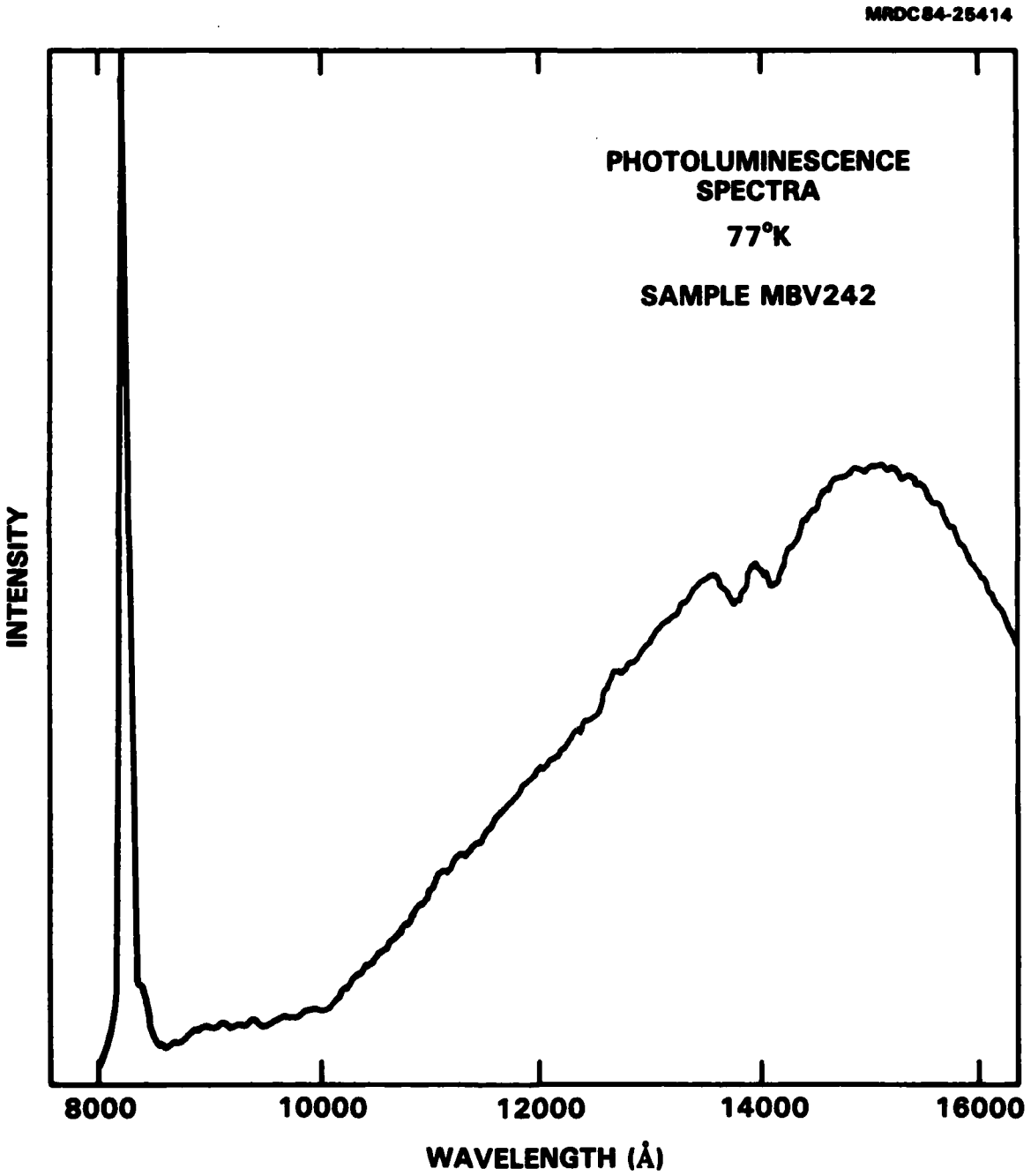

Fig. 21 Photoluminescence spectra, sample MBV 242.

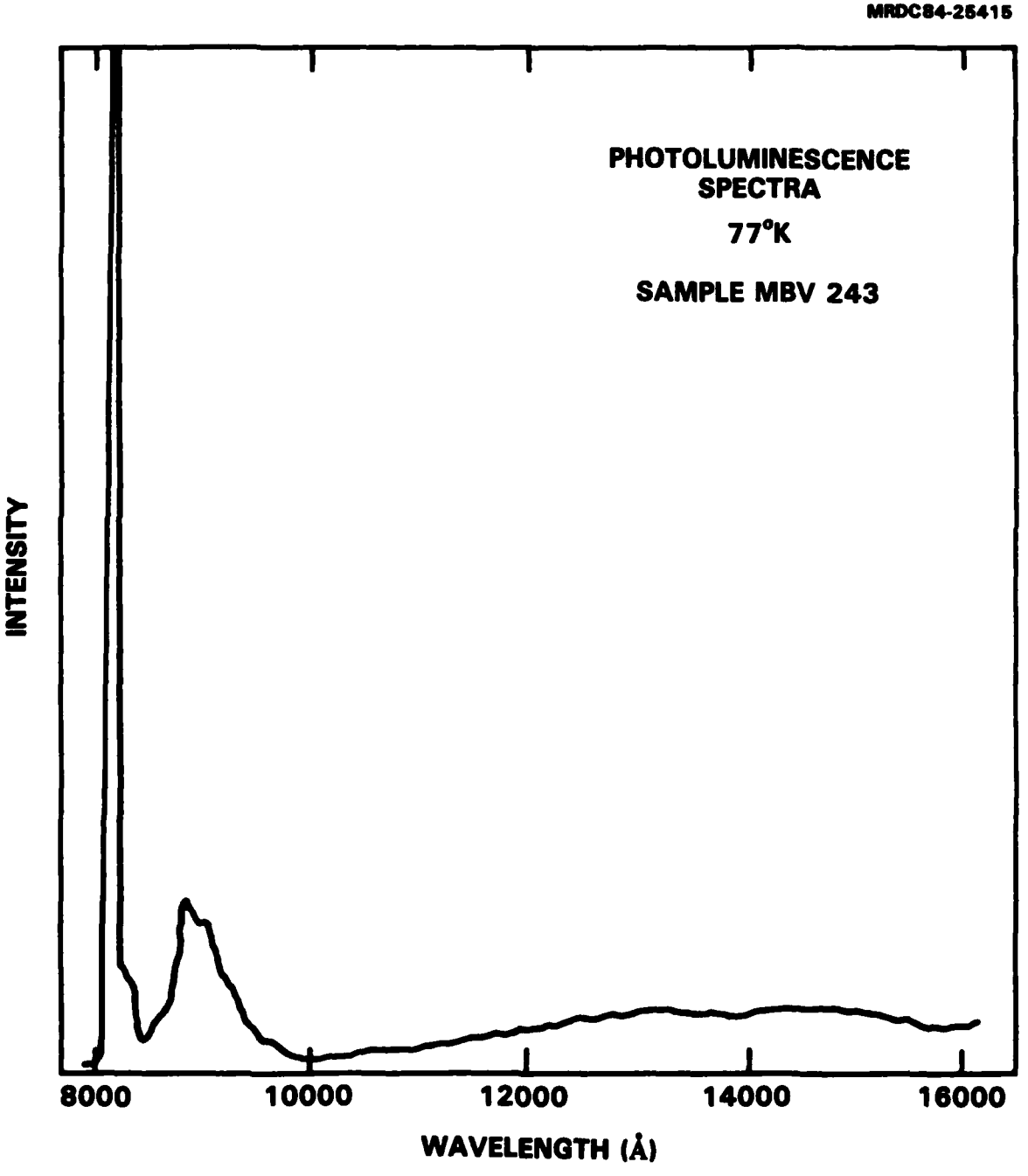

Fig. 22 Photoluminescence spectra, sample MBV 243.

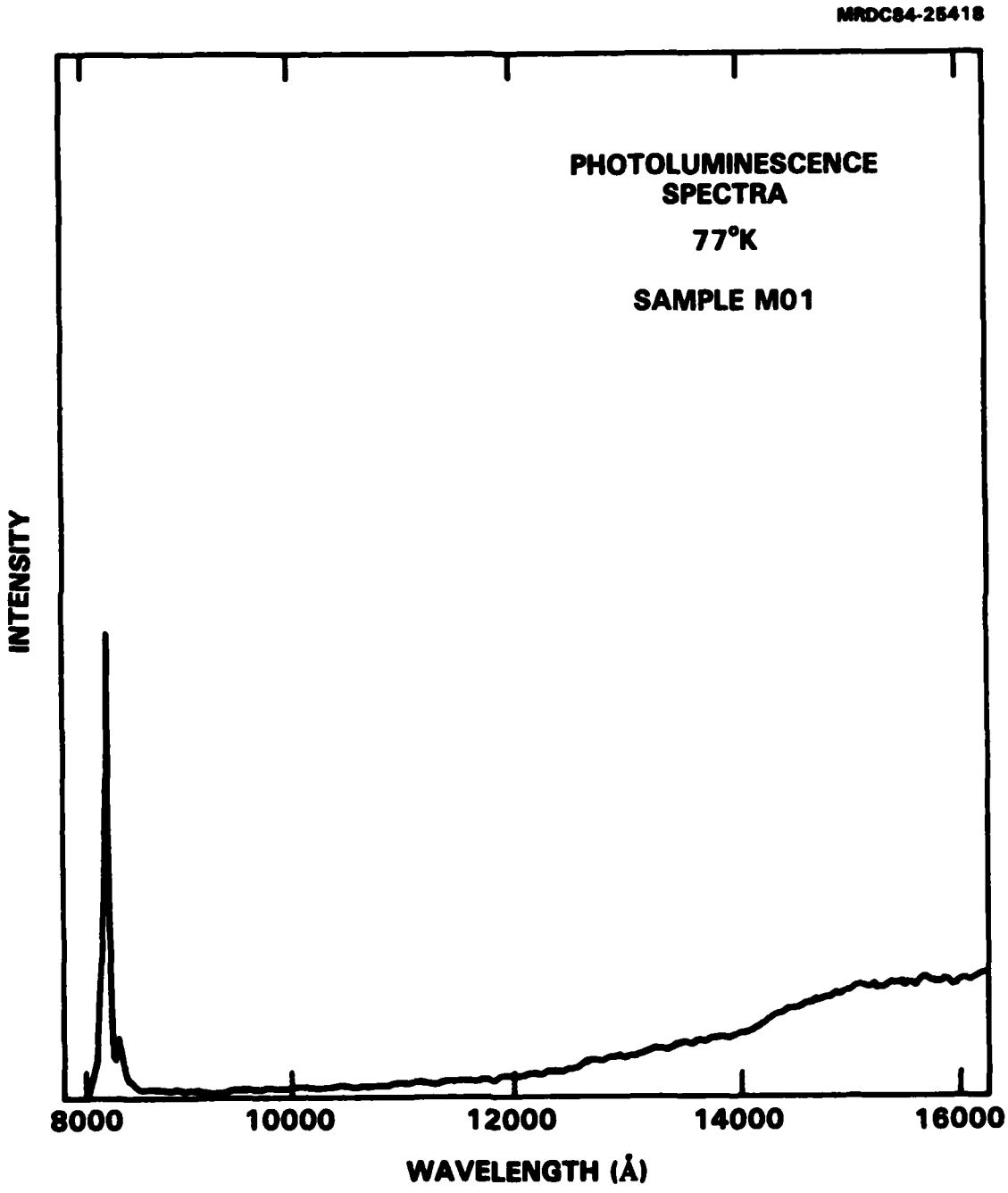

Fig. 23 Photoluminescence spectra, sample M01.

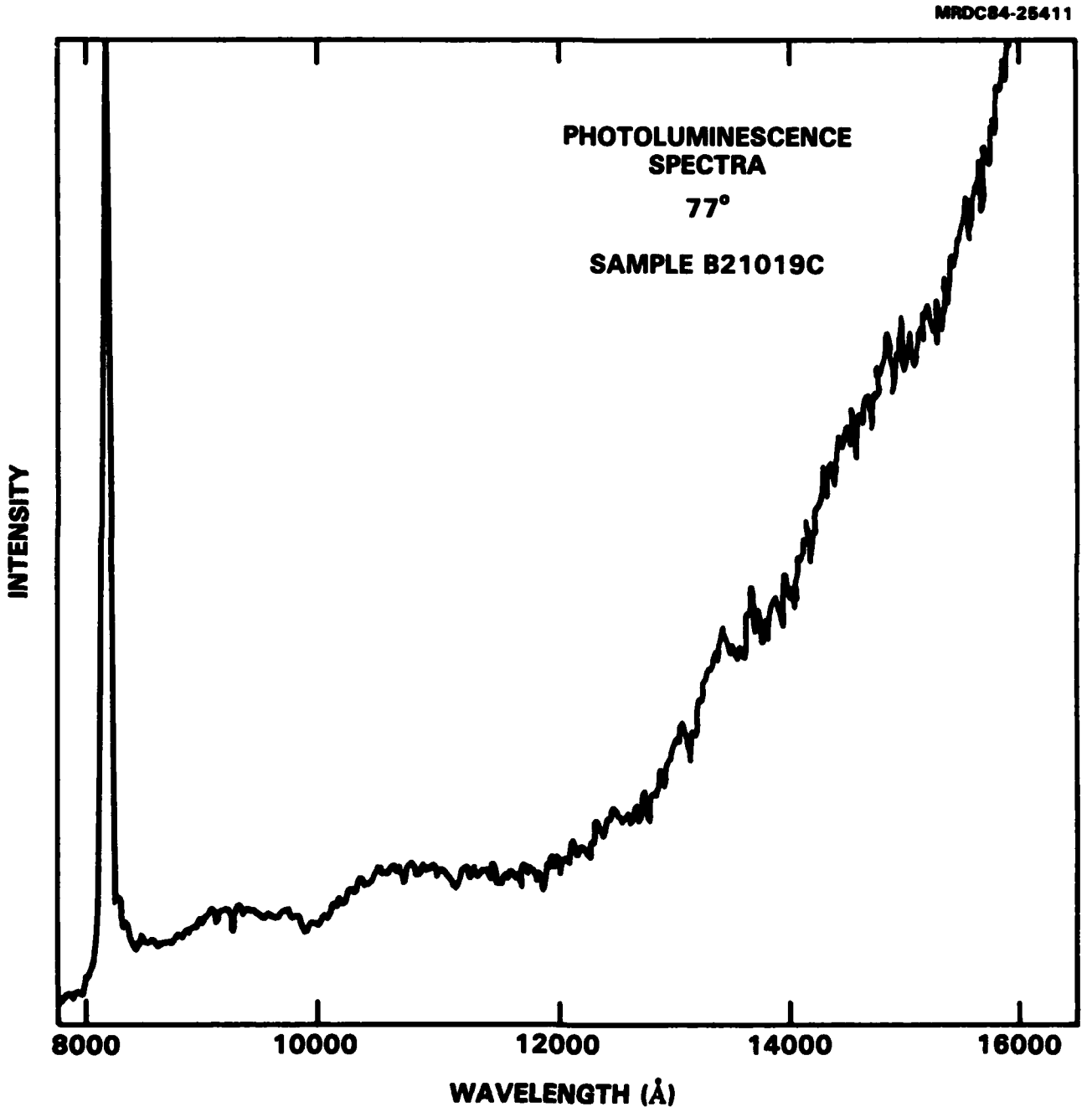

Fig. 24 Photoluminescence spectra, sample B21019C.

band may be associated with residual oxygen donors. Such donors might be expected to occur in MBE growth from residual contamination of the growth chamber. Luminescence associated with oxygen donors has not been unambiguously determined in the literature and hence any such identification should be considered uncertain. The luminescence of the MOCVD material typically only shows the presence of a broad luminescence band. This band peaks at wavelengths beyond 1.6 μm and is similar in appearance to the band observed in the substrate material. Hence, it is likely that this band may be associated with the deep donor EL2 which has been consistently observed in doped MOCVD material.

An attempt was made to quantitatively compare relative luminescence intensities with growth parameters in the MOCVD and MBE material. We did not observe any correlations.

4.0 IMPLANT STUDIES

Selected samples were implanted with Be and Se and annealed to establish the suitabilty of the material for ion implantation and related processing. Prior to anneal, the samples were coated with sputterd Si_3N_4. The implant activation was measured using C-V profiling and sheet resistance measurements. Control samples of undoped LEC substrate material were used to isolate processing induced variations in implant activation.

Of the nine MOCVD and nine MBE samples grown, all showed activation near 100% for Be implantation. However, all the samples showed negligible acivation for Se implantation. The Se implantation was repeated for a second time and some of the samples showed activation. The degree of fluctuation was highly variable. A control sample of substrate material showed normal activation in both cases. Typically, such studies have shown in the past that activation varies by less than 10% for suitably qualified material. Hence, the highly variable nature of the activation was unexpected.

In order to determine the mechanism by which compensation was occuring in the implanted epilayer material, SIMS and photoluminescence measurements were made on selected samples. Representative data is shown in Figs. 25 - 28 and Figs. 29 and 30 for these measurements. The SIMS measurements show large quantities of transition metals and contaminants in the surface regions of the epilayers which have been implanted. The photoluminescence spectra shows two intense bands peaked at 9100 and 1.25 m, which have previously been identified with copper-related acceptor levels. Since the luminescence is much more intense than in the as-grown epilayer or substrate material, we must assume that the source of copper is the processing environment and not the substrate or epilayer growth systems. This luminescence is typically very weak when the substrate material is implanted and annealed.

The most likely reason for this behavior is that macroscopic surface defects in the epilayer material induce pinholes in the Si_3N_4 capping layer. The surface morphology of the starting LEC material is considerably better than

the epilayer material. Hence the LEC substrate material would be less susceptible to this type of pinhole formation.

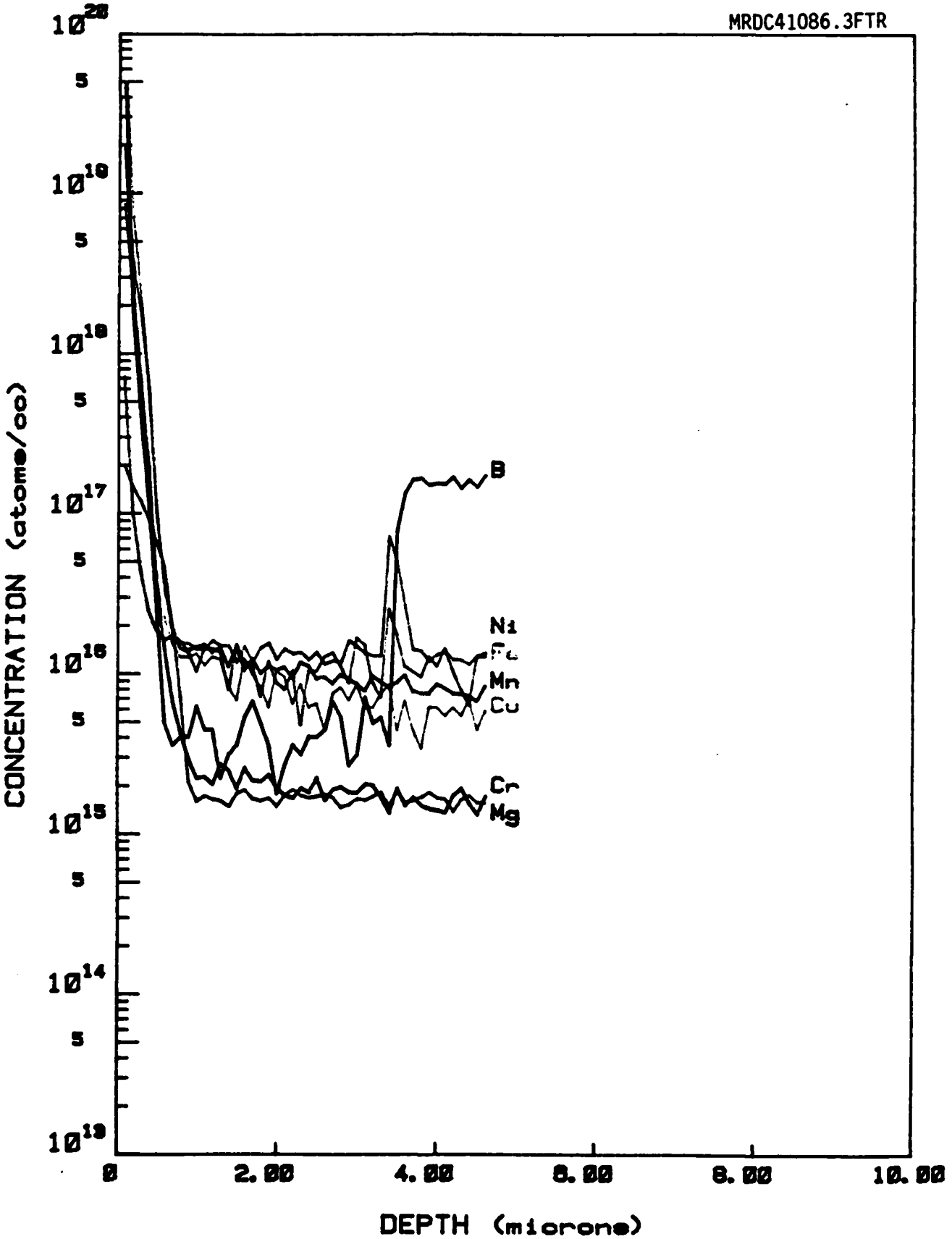

Fig. 25 SIMS profile, sample MBV 215 with Se implant.

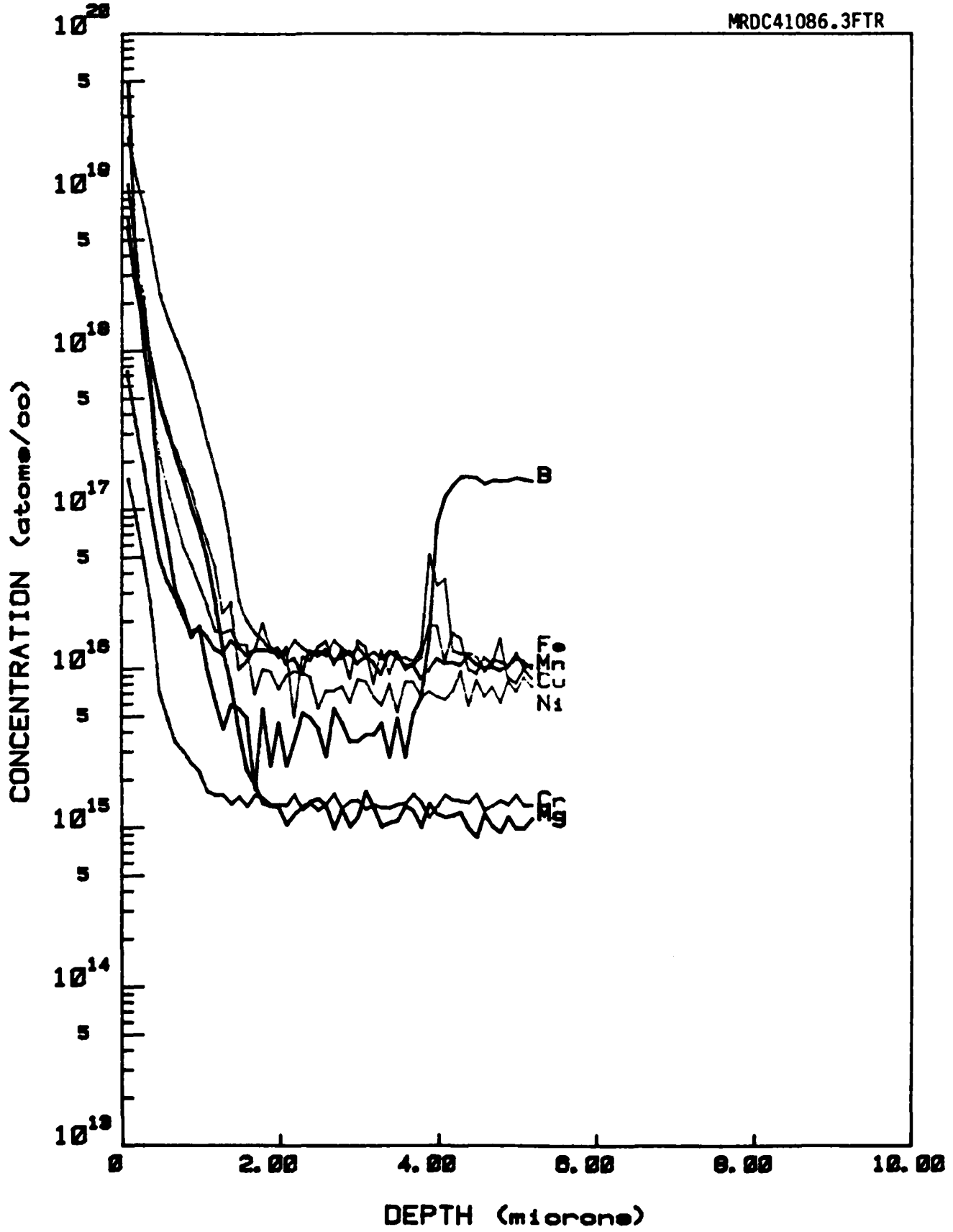

Fig. 26 SIMS profile, sample MBV 243 with Se implant.

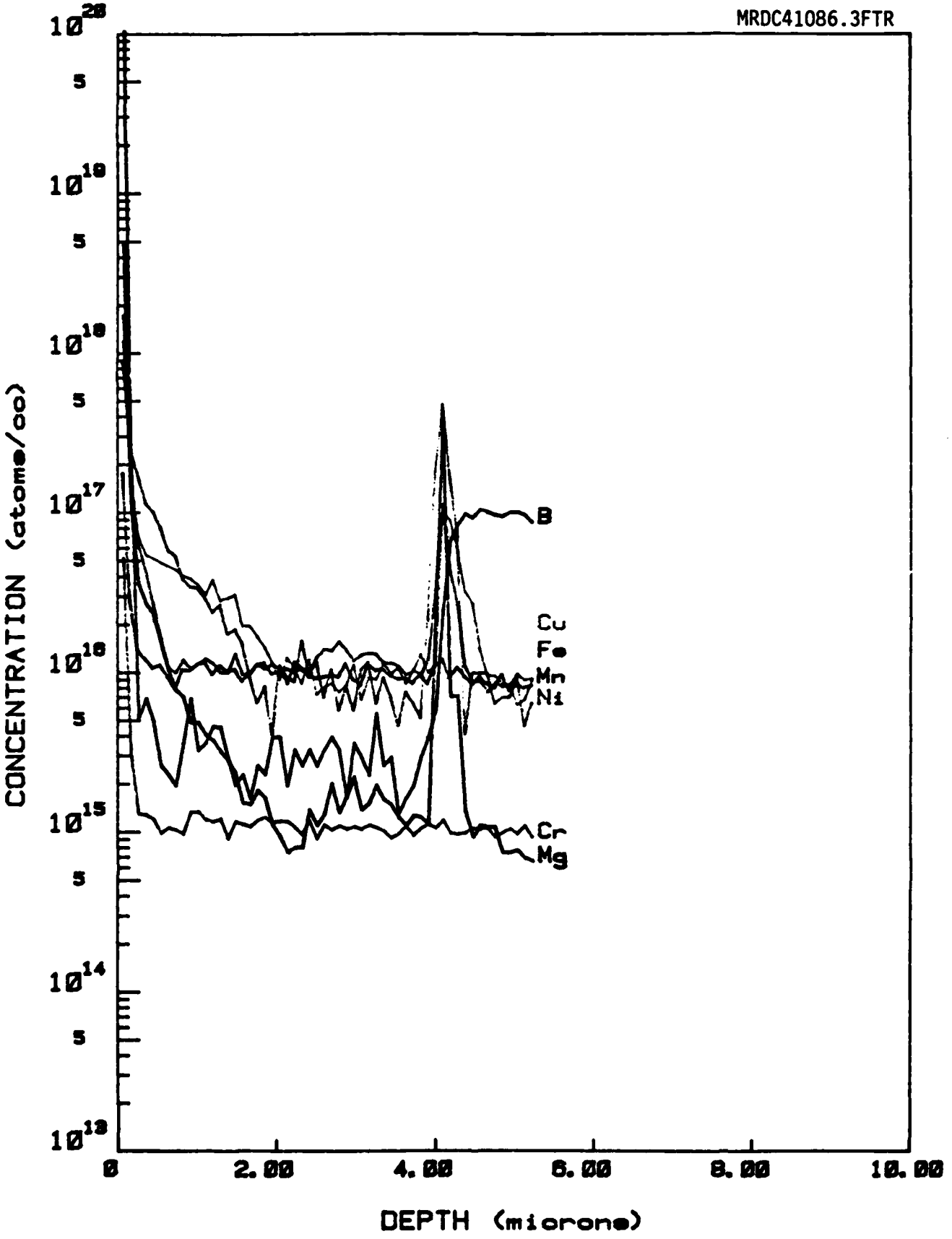

Fig. 27 SIMS profile, sample B30120B with Se implant.

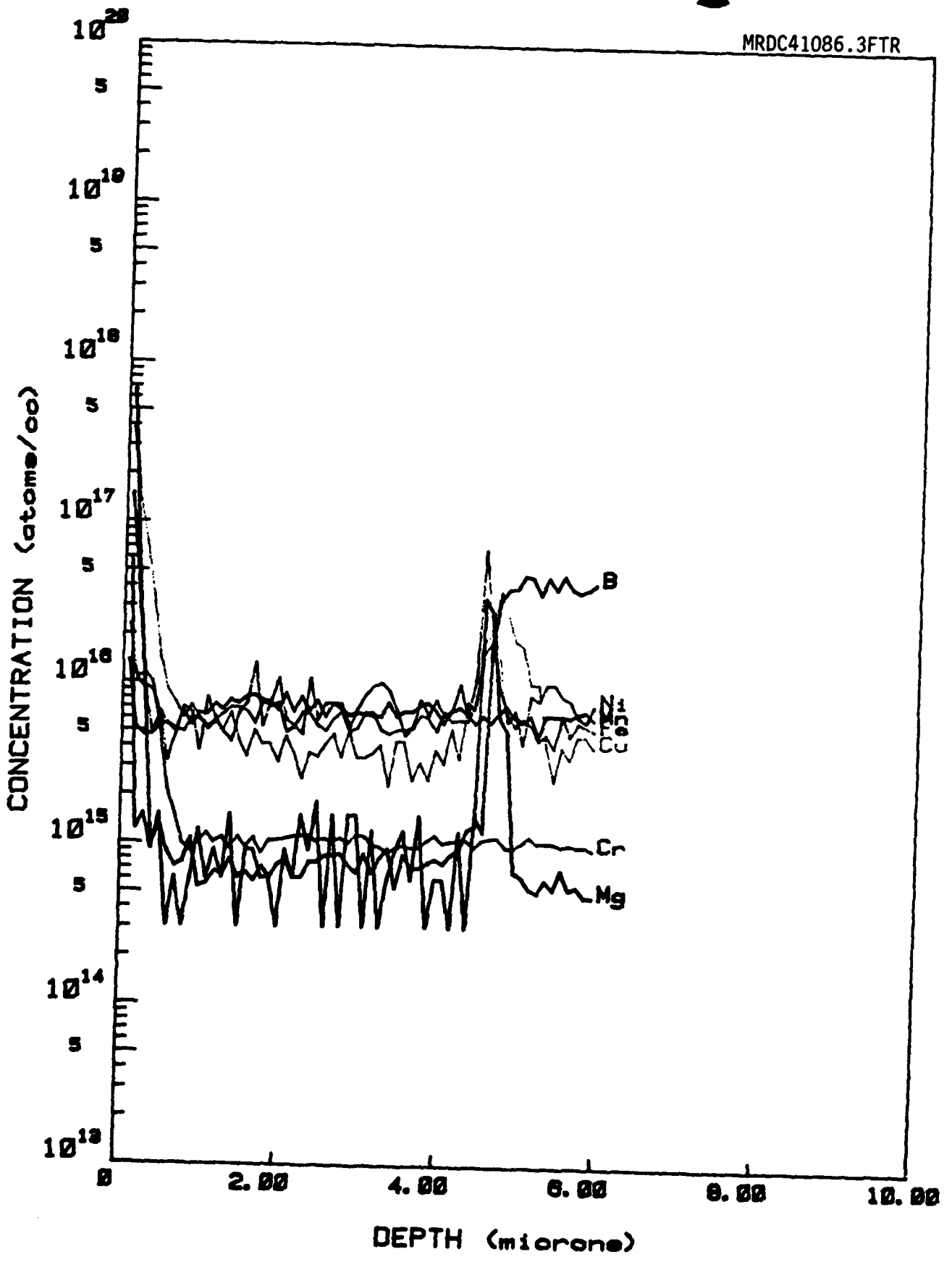

Fig. 28 SIMS profile, sample B30228B with Se implant.

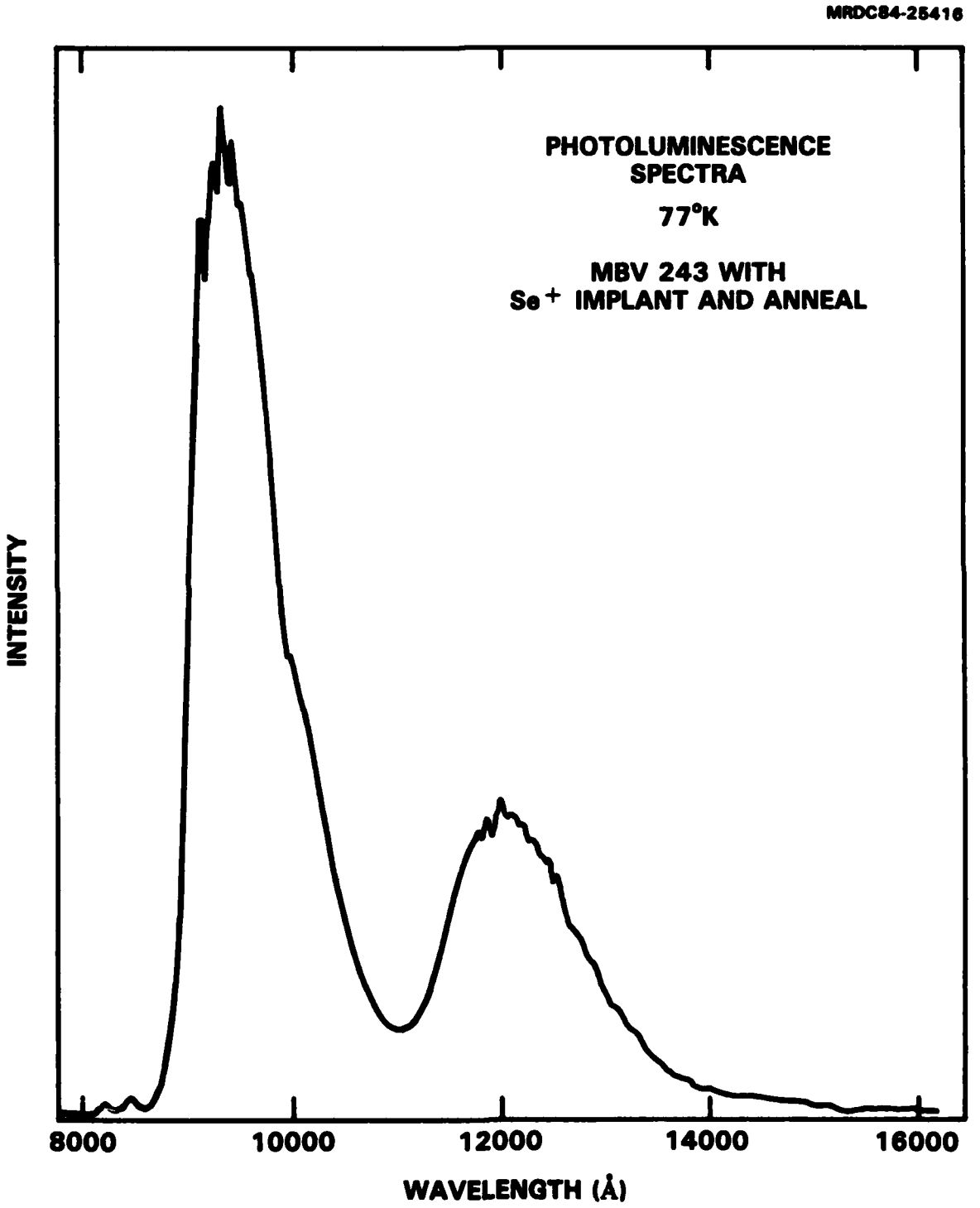

Fig. 29 Photoluminescence spectra, sample MBV 243 with Se implant.

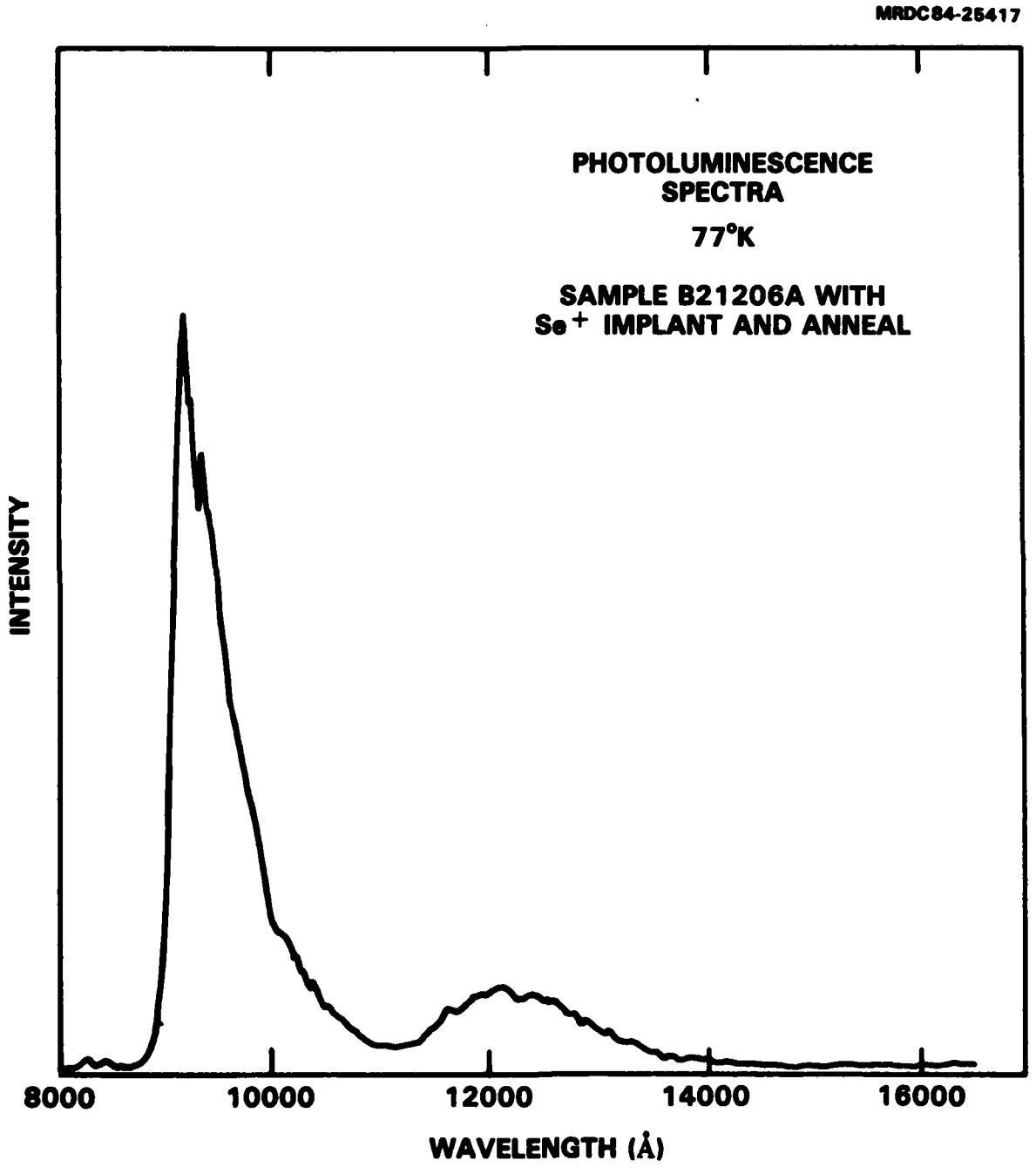

Fig. 30 Photoluminescence spectra, sample B21206A with Se implant.

5.0 CONCLUDING REMARKS

In this program we have produced epitaxial layers grown by MBE, MOCVD and VPE for comparison. These layers have been characterized using SIMS, Hall measurements, some photoluminescence studies and transport technique such as PITS, DLTS, and infrated photoresponse. We found no evidence of systematic variations in conductivity or deep level content which depend on the growth conditions.

We did observe that the surface morphology and macroscopic surface defect density did depend on the growth conditions in some cases (Section 3.0) and that these surface morphology variations may have an effect on the subsequent ion implantation and anneal processing when compared to the starting substrate material (Section 4.0).

Both MBE and MOCVD samples show evidence of deep level recombination in some photoluminescence. However, since we did not observe any systematic dependence of this photoluminescence or of any specific trapping centers in transport measurements on the growth conditions, these levels are probably of extrinsic origin. The fact that we observe Fe, Mg (C?) and other elements accumulating at the epilayer/substrate interface in some instances suggests that initial surface preparation is very important in determining the impurity content in the epilayer material. Other extrinsic contaminants probably include C and O contaminants from residual gases in the growth system.

The purity obtained from each of the growth methods was comparable as indicated by electrical measurements with typical impurity and defect concentrations of 10^{13}-10^{14} cm^{-3}. This value is sufficiently low that further reduction only has a small effect on mobility enhancement. Also for layers < 2 m in thickness high sheet resistance is obtained (Section 3.3.1) for enhanced isolation. It should be pointed out, however, that although these layers have high ohmic resistance, they may be particularly susceptible to space charge current in the trap filled limit since the number of traps in the epilayer is extremely low.

The differences between MBE and MOCVD growths were indicated principally by the residual defect species observed in photoluminescence. In some of the MBE samples Cu-related defect luminescence was observed. In one of the MOCVD samples, deep level luminescence is anomolously intense compared to the others. MOCVD samples also showed larger numbers of trapped impurities at the epilayer/substrate interface.